TopBP1/Dpb11 binds DNA anaphase bridges to prevent genome instability

Susanne M. Germann, Vera Schramke, Rune Troelsgaard Pedersen, Irene Gallina, Nadine Eckert-Boulet, Vibe H. Oestergaard, and Michael Lisby

Department of Biology, University of Copenhagen, Ole Maaloeesvej 5, DK-2200 Copenhagen N, Denmark

DNA anaphase bridges are a potential source of genome instability that may lead to chromosome breakage or nondisjunction during mitosis. Two classes of anaphase bridges can be distinguished: DAPI-positive chromatin bridges and DAPI-negative ultrafine DNA bridges (UFBs). Here, we establish budding yeast *Saccharomyces cerevisiae* and the avian DT40 cell line as model systems for studying DNA anaphase bridges and show that TopBP1/Dpb11 plays an evolutionarily conserved role in their metabolism. Together with the single-stranded DNA binding protein RPA, TopBP1/Dpb11 binds to UFBs, and depletion of TopBP1/Dpb11 led to an accumulation of chromatin bridges. Importantly, the NoCut checkpoint that delays progression from anaphase to abscission in yeast was activated by both UFBs and chromatin bridges independently of Dpb11, and disruption of the NoCut checkpoint in Dpb11-depleted cells led to genome instability. In conclusion, we propose that TopBP1/Dpb11 prevents accumulation of anaphase bridges via stimulation of the Mec1/ATR kinase and suppression of homologous recombination.

Introduction

Faithful segregation of the genetic material during cell division is crucial for maintenance of genome integrity. The two complements of the genome must be disentangled before migration into the daughter cells in mitosis. This is a topologically challenging process because sister chromatids are frequently catenated or connected by hemicatenanes at the G2–M transition (Lucas and Hyrien, 2000; Lopes et al., 2003; Wellinger et al., 2003; Liberi et al., 2005; Johnson et al., 2009). As a consequence, the separating sister chromatids are often connected by DNA bridges in anaphase. A subset of these DNA anaphase bridges has been linked to chromosomal fragile sites in human cells (Chan et al., 2009; Lukas et al., 2011). Fragile sites are prone to chromosome breakage, deletion, and translocation, and are often associated with cancer and other genetic diseases (Durkin and Glover, 2007; Gandhi et al., 2010).

DNA anaphase bridges can be divided into two classes (Kaulich et al., 2012): chromatin bridges that can be visualized by DAPI staining, and ultrafine DNA bridges (UFBs; Chan et al., 2007), which are refractory to DAPI staining. In mammalian cells, UFBs are bound by the PICH, BLM, and FANCM helicases, and a subset of UFBs are marked by the Fanconi anemia (FA) proteins, FANCD2 and FANCI, which localize to the termini of these UFBs (Chan et al., 2009; Naim and Rosselli, 2009; Vinciguerra et al., 2010). A subset of BLM-stained UFBs also contain replication protein A (RPA), indicating that some bridges are at least partially single stranded (Chan and Hickson, 2009). In contrast to UFBs, chromatin bridges contain nucleosomes and other chromatin components.

Several models have been suggested to explain the origin of UFBs (Chan and Hickson, 2011). The FA-negative UFBs are the most abundant in unperturbed cells. They originate primarily from centromeric regions and are induced by topoisomerase II inhibition, suggesting that they reflect catenated sister chromatids. The FA-positive UFBs are rare in unperturbed cells, are induced by inhibition of DNA replication, and originate

S.M. Germann, V. Schramke, and R.T. Pedersen contributed equally to this paper.

Correspondence to Michael Lisby: mlisby@bio.ku.dk

S.M. Germann's present address is Centre for Healthy Aging, Faculty of Health Sciences, University of Copenhagen, DK-2200 Copenhagen N, Denmark.

V. Schramke's present address is Department of Protein Expression, Novo Nordisk A/S, DK-2760 Maaloev, Denmark.

Abbreviations used in this paper: AID, auxin-inducible degron; APH, aphidicolin; ATRi, ATR inhibitor; EdU, 5-ethynyl-2′-deoxyuridine; FA, Fanconi anemia; HR, homologous recombination; MMS, methyl methanesulfonate; RPA, replication protein A; SPB, spindle pole body; TFP, mTurquoise2; UFB, ultrafine bridge.

Supplemental material can be found at:
http://doi.org/10.1083/jcb.201305157

The Rockefeller University Press $30.00
J. Cell Biol. Vol. 204 No. 1 45–59
www.jcb.org/cgi/doi/10.1083/jcb.201305157

primarily at common fragile sites (Chan et al., 2009; Naim and Rosselli, 2009). Although BLM is known to process DNA recombination structures, UFBs are unlikely to reflect recombination intermediates such as Holliday junctions because FANCD2 foci and UFB formation are independent of the RAD51 recombinase (Chan et al., 2009; Lahkim Bennani-Belhaj et al., 2010).

Chromosomal fragile sites are often marked by 53BP1 in G1 when cells have been exposed to mild replication stress in the previous S phase, indicating that these sites may represent single-stranded gaps originating from incomplete DNA replication (Lukas et al., 2011). The latter study suggested that no checkpoint exists to detect and prevent onset of mitosis in the presence of unreplicated regions of the genome. However, in yeast, lagging chromatin across the spindle midzone, which could be a consequence of unreplicated DNA, was shown to activate a NoCut checkpoint that delays abscission until the sister chromatids are fully segregated (Mendoza et al., 2009). The NoCut checkpoint requires the Ipl1/Aurora B kinase, the spindle-associated factor Slk19, and the Ahc1 histone acetyltransferase (Mendoza et al., 2009). Similarly, in human cells Aurora B was shown to delay abscission in cells with chromosome bridges (Steigemann et al., 2009).

In this study, we report that the DNA damage checkpoint, replication and repair protein Dpb11 localizes to UFBs in budding yeast along with Sgs1-Top3 (BLM-TopoIIIα), RPA, and the checkpoint protein Ddc2 (ATRIP). We also show that the vertebrate orthologue of Dpb11, TopBP1, colocalizes with PICH and RPA at a subset of UFBs in chicken DT40 cells. Depletion of Dpb11 or TopBP1 leads to an accumulation of chromatin bridges but a reduction in the frequency of long UFBs. UFBs in yeast are sensed by the NoCut checkpoint to delay cytokinesis, and simultaneous disruption of the NoCut checkpoint and depletion of Dpb11 leads to a synergistic increase in genome instability.

Results

Dpb11 localizes to ultrafine anaphase bridges in mitotic cells

We have recently reported the localization of Dpb11 to DNA double-strand breaks (Germann et al., 2011). In the course of this work, we noticed that Dpb11 localizes to a structure bridging the daughter and mother nuclei in 1–3% of cells in an asynchronous population (Fig. 1 A). When Dpb11 localization was monitored by time-lapse microscopy using 5-min intervals, spontaneous Dpb11 bridges were observed in 43% of anaphases ($n = 37$). Because this experiment was performed with a *tetO$_2$-DPB11-YFP* construct that overexpresses Dpb11 approximately fourfold compared with the native promoter (Germann et al., 2011), we confirmed that Dpb11 also forms anaphase bridges when expressed from its native promoter (Fig. 1 B). The majority (70–80%) of these bridges fail to stain with conventional DNA dyes (DAPI and Hoechst; Fig. 1, B, C, and F). Further experiments showed that Dpb11 bridges frequently (>80%) colocalize with Rfa1 (RPA; Fig. 1 C), suggesting that these structures at least partially consist of single-stranded DNA, similar to what has been reported for ultrafine DNA bridges in mammalian cells (Chan and Hickson, 2009). To further extend the comparison to mammalian UFBs, we tested the localization of Sgs1-Top3 to Dpb11 bridges. Live-cell imaging showed that Sgs1 and Top3 colocalize with Dpb11 bridges in a subset (60%) of mitotic cells (Fig. 1 D). In contrast, a range of chromatin-associated factors such as Hta1 (histone H2A), Htz1 (histone variant H2AZ), Rsc1 (RSC chromatin remodeling complex), Nhp10 (INO80 chromatin remodeling complex), and Nop1 (nucleolar protein) were generally absent from Dpb11-coated anaphase bridges, indicating that these structures are largely free of chromatin and do not represent the normally late-segregating nucleolus (Fig. 1, E and F; Torres-Rosell et al., 2004).

Yeast anaphase tubes contain DNA bridges bound by Dpb11

In contrast to vertebrate cells, the yeast nuclear envelope remains intact during mitosis, causing the nuclear membrane to be stretched into a narrow tube during anaphase as visualized by the nuclear pore complex subunit Nup49 (Fig. 2 A). Therefore, any bridge-like localization of a nuclear protein at this phase of the cell cycle could simply reflect the nucleoplasm contained within the anaphase tube. Indeed, red fluorescent protein tagged with a nuclear localization signal (NLS-RFP) exhibits a bridge-like localization coinciding with Dpb11 bridges (Fig. 2 A). To determine which of the proteins within anaphase bridges are bound to DNA, we performed time-lapse microscopy of dividing Dpb11-YFP cells expressing NLS-RFP and Spc110-CFP to mark the nucleoplasm and spindle pole body (SPB), respectively (Fig. 2 B). Resolution of the Dpb11 bridge before the NLS-RFP marker was observed in 43% of anaphases examined ($n = 37$), indicating that upon relaxation of the mitotic spindle, the Dpb11 bridge is resolved, whereas the NLS-RFP marker remains in the anaphase tube until nuclear division. These data imply that Dpb11 is associated with DNA at the anaphase bridge. To directly demonstrate the presence of DNA in the anaphase bridges, we constructed a strain that allows incorporation of the nucleoside analogue 5-ethynyl-2′-deoxyuridine (EdU; Viggiani and Aparicio, 2006). This thymidine analogue can be conjugated to a fluorescently labeled azide. Using this technique, we detected the DNA in Hoechst-negative anaphase bridges (Fig. 2 C). Subsequent immunostaining for Dpb11-YFP was incompatible with preservation of the UFBs, but similar to Dpb11-bound UFBs (see following paragraph), the EdU-labeled bridges were induced by mild replication stress (20 mM hydroxyurea), indicating that Hoechst-negative Dpb11 UFBs and EdU-labeled bridges reflect the same structure (Fig. 2 D). Two additional observations were consistent with this conclusion. First, Rfa1 was also bound to UFBs (Fig. S1). Second, disappearance of Dpb11 from bridges coincided with relief of spindle tension, not nuclear division, as seen by the change of SPB movement from poleward to random (Fig. 2, B and E). Furthermore, in cells without a Dpb11 bridge, nuclear division takes place when the SPBs are separated by 4–6 µm, whereas cells containing a Dpb11 bridge exhibit SPB distances of up to 9 µm with a peak at 7 µm (Fig. 2 F), indicating that nuclear division is delayed in cells containing Dpb11 anaphase bridges.

Dpb11 bridges are induced by DNA replication and topological stress

To determine the effect of DNA replication stress on the formation of Dpb11 anaphase bridges, we exposed cells to 0.03%

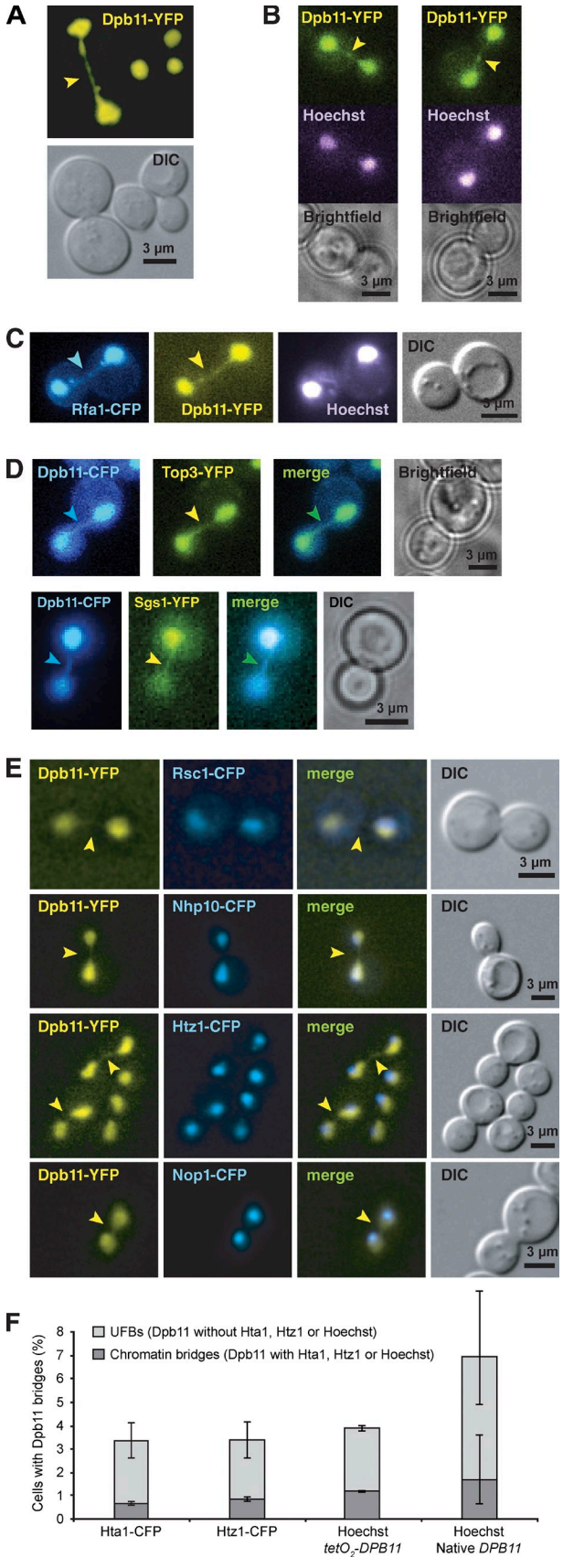

Figure 1. **Dpb11 associates with chromatin-free anaphase bridges in mitotic cells.** The localization of proteins of interest was determined in haploid cells during the exponential growth phase by fluorescence microscopy and differential interference contrast. Arrowheads mark bridges. (A) Dpb11 forms bridge-like structures in mitotic cells. Cells expressing Dpb11-YFP from the *Tet-Off* promoter (ML535-5D) were analyzed. (B) Dpb11 under the control of its native promoter also forms ultrafine anaphase bridges. Cells expressing Dpb11-YFP (ML253) from its native promoter were analyzed after Hoechst staining. (C) Dpb11 and Rfa1 colocalize at UFBs. Cells expressing Dpb11-YFP and Rfa1-CFP (SMG216-10A) were analyzed after Hoechst staining. (D) Dpb11 bridges colocalize with Top3 and Sgs1 bridges. Cells coexpressing Dpb11-CFP with Top3-YFP (SMG247-4A) or YFP-Sgs1 (SMG258-10A) were analyzed. (E) Dpb11 bridges rarely colocalize with chromatin-associated factors or rDNA-binding proteins. Cells expressing Dpb11-YFP and Rsc1-CFP (SMG220-15A), Nhp10-CFP (SMG221-15D), or Htz1-CFP (SMG219-5D), or cells (ML533) expressing Dpb11-YFP transformed with a plasmid expressing Nop1-CFP (pWJ1299) were analyzed. (F) Dpb11 bridges are predominantly Hoechst and chromatin negative. UFBs and chromatin bridges were counted as Dpb11-YFP bridges that do or do not colocalize with Hta1-CFP (VS23-1B), Htz1-CFP (SMG219-5D), or Hoechst (ML533 and ML253), respectively. Error bars represent 95% confidence intervals.

methyl methanesulfonate (MMS), which blocks replication fork progression through DNA methylation (Tercero and Diffley, 2001). Exposure to MMS led to a transient accumulation of Dpb11 bridges (Fig. 3 A), supporting the notion that DNA replication stress leads to formation of DNA anaphase bridges also in yeast. To monitor the formation of Dpb11 bridges during unchallenged DNA replication, we performed an arrest-release experiment, where Dpb11-YFP localization was monitored after release from α-factor–mediated G1 arrest (Fig. 3 B). In this experiment, Dpb11 bridges appeared at 60 min after release, accumulated until late anaphase at 90 min, and finally disappeared at 120 min, when most of the cells had completed nuclear division (Fig. 3 C). This result indicates that Dpb11 anaphase bridges form in early anaphase and persist until late mitosis. This conclusion was further supported by time-lapse microscopy, which demonstrated that Dpb11 bridges progressively elongate through anaphase. Cells with long anaphase bridges recovered and progressed into the next cell cycle as evidenced by rebudding of both the mother and daughter cell with the same frequency as cells with no bridges or short bridges (Fig. S2).

Top2 catalyzes the decatenation of duplex DNA. To test if catenated chromatids can also lead to anaphase bridges in yeast, we measured Dpb11 bridges in a conditional *top2-1* mutant (Brill et al., 1987). Even at the permissive temperature of 25°C, we observed a dramatic increase in the percentage of cells with Dpb11 bridges (Fig. 3 D), indicating that Top2 activity plays a major role in removing anaphase bridges. Although the *top2-1* mutant exhibited a basal level of Hoechst-positive chromatin bridges comparable to wild type at the permissive temperature, these were strongly induced at the restrictive temperature (Fig. 3 D). Notably, MMS-induced replication stress and mutation of Top2 additively induced formation of Dpb11-bound anaphase bridges, indicating that topological and replication stress independently contribute to the formation of UFBs (Fig. 3 D). Consistent with a role for Top2 in decatenating intertwined sister chromatids, Top2 itself localized predominantly to Hoechst-negative anaphase bridges (Fig. 3 E). The higher frequency of Top2 bridges (13%) observed in comparison to Dpb11 bridges (4%) could indicate that the function of the Top2-CFP fusion is partially compromised and/or that Top2

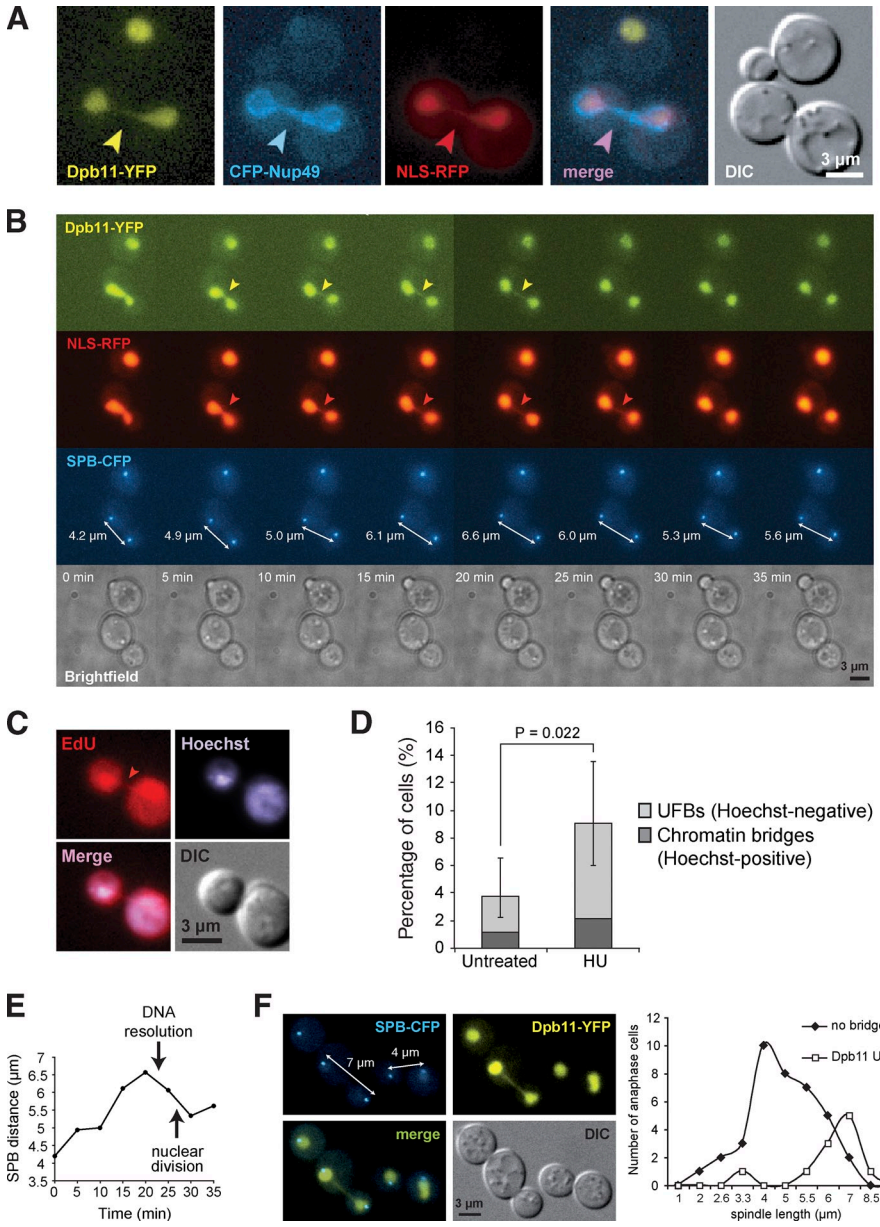

Figure 2. **Yeast anaphase tubes contain DNA bridges bound by Dpb11 that delay nuclear division.** (A) Dpb11 anaphase bridges are contained within an anaphase tube. Cells (ML533) expressing Dpb11-YFP, CFP-Nup49 (pWJ1323), and NLS-RFP (pKW1219) were grown in SC-His-Leu medium with 100 µg/ml adenine. (B) Dpb11 is bound to DNA in anaphase bridges. Cells (ML628) expressing Dpb11-YFP, Spc110-CFP, and NLS-RFP were analyzed by time-lapse microscopy. Resolution of the Dpb11 bridge before the NLS-RFP marker was observed in 43% of anaphases examined (n = 37). (C) Hoechst-negative anaphase bridges contain DNA. Cells (VS28) were grown for 3 h in SC+Ade medium with 20 µM EdU before fixation and Hoechst staining. (D) Hoechst-negative EdU-positive anaphase bridges are induced by hydroxyurea. Cells (VS28) were labeled with EdU for 3 h before treatment with 20 mM hydroxyurea (HU) for 1 h and subsequently fixed and stained with Hoechst. Error bars represent 95% confidence intervals. (E) Resolution of Dpb11 bridges is coincidental with relaxation of the mitotic spindle. The distance between the SPBs (Spc110-CFP) in B was measured in three dimensions (3D) and plotted as a function of time. (F) Relationship between spindle length and Dpb11 bridges. Cells (VS3-7A) expressing Dpb11-YFP and Spc110-CFP (SPB) were imaged. The distance between the SPBs was measured in 3D and the cells scored for Dpb11 bridges. The median spindle length observed for Dpb11 bridge–negative and –positive cells was 4.7 µm and 7.0 µm, respectively. Only Hoechst-negative Dpb11 bridges were counted.

recognizes other kinds of anaphase bridges than those bound by Dpb11. Notably, the majority of Top2 bridges (73%) are also bound by Dpb11 (Fig. 3 F).

The Smc5–Smc6 complex collaborates with topoisomerases to regulate the topological state of chromosomes presumably by sequestering sister chromatid intertwining behind the DNA replication fork (Kegel et al., 2011). We therefore examined a conditional *smc6-9* mutant for the formation of Dpb11 bridges. At the restrictive temperature, *smc6-9* cells exhibit a dramatic increase in the percentage of cells with predominantly Hoechst-negative Dpb11 bridges, indicating that the Smc5–Smc6 complex contributes to the suppression of UFB formation (Fig. 3 G).

Dissolution of hemicatenanes and/or Holliday junctions by BLM-TopoIIIα-RMI1/2 was suggested to contribute to resolution of UFBs in mammalian cells, because BLM-deficient cells exhibit elevated levels of PICH bound UFBs (Chan et al., 2009). To test whether Sgs1 plays a similar role in yeast, we determined the percentage of cells with Dpb11 bridges in an *sgs1Δ* mutant. In *sgs1Δ* cells the number of chromatin bridges increased, while wild-type levels of UFBs were observed (Fig. 4 A). Taken together, these results show that both DNA replication problems and topological stress are sources of DNA anaphase bridges in yeast.

Homologous recombination promotes the formation of chromatin bridges

Another potential source for interlinked sister chromatids is homologous recombination (HR) intermediates. Using mammalian cells it was found that UFB formation is independent of or even increased in the absence of functional RAD51 recombinase (Chan et al., 2009; Lahkim Bennani-Belhaj et al., 2010; Laulier et al., 2011). Similarly, we found that both spontaneous and MMS-induced Hoechst-negative Dpb11 bridges in yeast were largely independent of the Rad52, Rad51, and Rad54

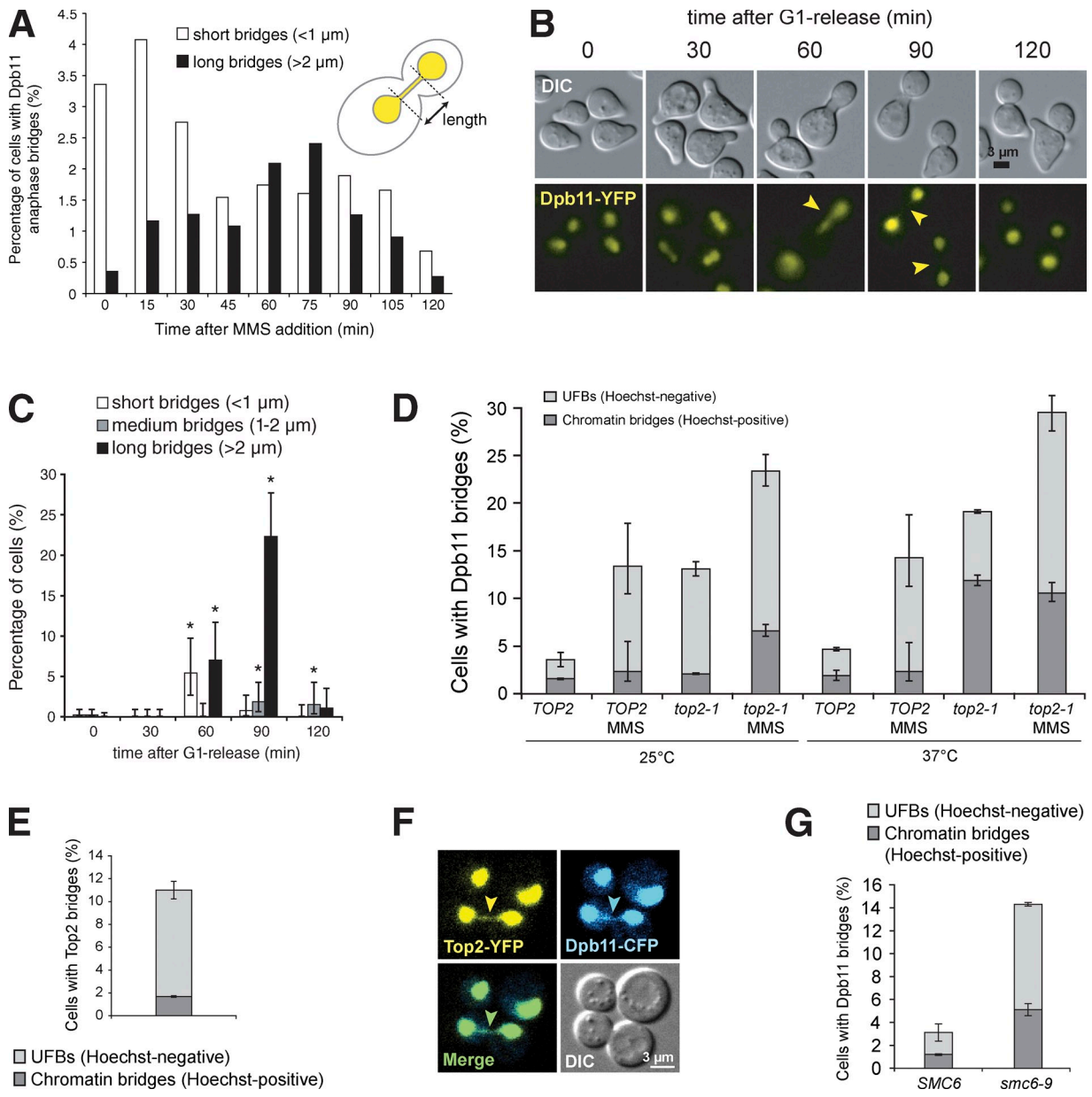

Figure 3. **Dpb11 bridges are induced by compromised DNA replication or sister chromatid decatenation.** (A) Dpb11 bridges are induced by replication stress. Cells expressing Dpb11-YFP (ML533) were analyzed at the indicated time points after treatment with MMS (0.03%). For quantification, 300–700 cells were analyzed per time point. Bridges are defined as short bridges (<1 µm) or long bridges (>2 µm). (B) Dpb11 bridges form at the metaphase-to-anaphase transition (between 60 and 90 min after G1 release). Cells expressing Dpb11-YFP (ML533) were arrested in G1 phase with α-factor for 2.5 h, and subsequently released into fresh medium without α-factor. Pictures were taken at the indicated time points after G1 release. The length of bridges was measured as in A. (C) Quantitation of anaphase bridges after release from G1 arrest. For each time point in B, 150–350 cells were analyzed. Asterisk indicates a P value of <0.05 compared with time-point zero. (D) Dpb11 bridges accumulate in a *top2-1* mutant. A temperature-sensitive *top2-1* mutant (VS11-13D) and its corresponding *TOP2* wild type (ML533) were examined for Dpb11-YFP bridges at the permissive temperature (25°C) or after incubation at the restrictive temperature (37°C) for 2 h. Indicated samples were treated with 0.03% MMS for 70 min. (E) Top2 localizes to UFBs. Cells expressing Top2-CFP (VS21) were stained with Hoechst and examined for Top2 bridges. (F) Top2 and Dpb11 colocalize on anaphase bridges. Cells expressing Dpb11-CFP and Top2-YFP (VS22-7B) were analyzed. (G) Dpb11 bridges accumulate in an *smc6-9* mutant. A temperature-sensitive *smc6-9* mutant (SMG266-6D) and its corresponding *SMC6* wild type (ML533) were examined for Dpb11-YFP bridges after incubation at the restrictive (37°C) temperature for 2 h. Error bars represent 95% confidence intervals.

recombination proteins (Fig. 4, A and B), which is also consistent with our observation that Rad52 binds only to chromatinized Dpb11 bridges (see following paragraph). Interestingly, the chromatin bridges observed in the *sgs1* mutant were dependent on HR, indicating that hemicatenated DNA might induce illegitimate recombination leading to formation of chromatin bridges or that Sgs1 suppresses chromatin bridges by dissolution of double-Holliday junctions. Consistent with a role of HR in the formation of Dpb11-bound chromatin bridges, overexpression of Rad51, but not of the catalytically inactive Rad51-K191A mutant, led to increased numbers of Dpb11-marked chromatin bridges (Fig. 4 C). To examine the impact of Dpb11 on anaphase bridges, we took advantage of the *Tet-Off* promoter (*tetO*$_2$) to shut off expression of Dpb11 by addition of doxycycline.

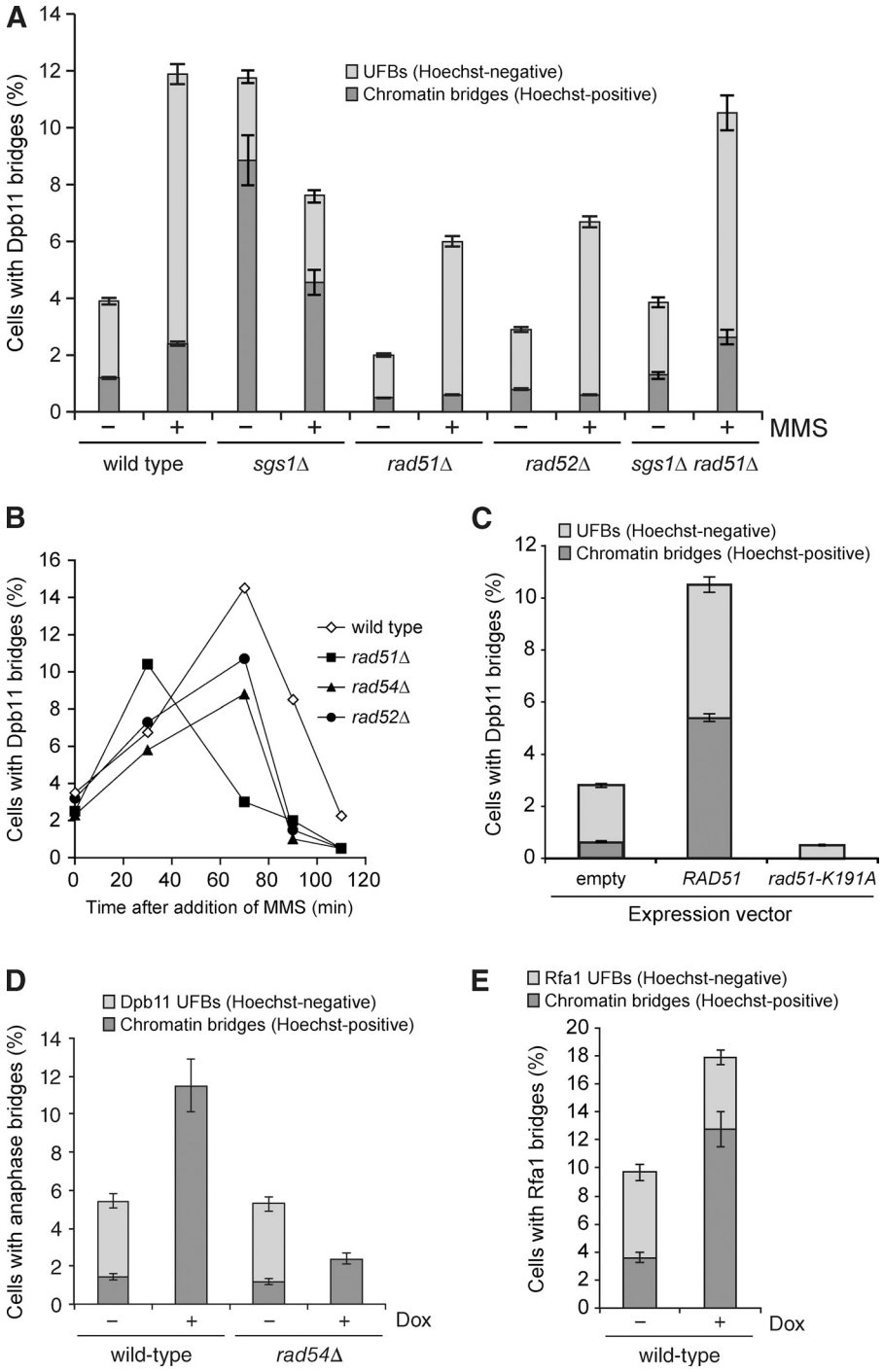

Figure 4. **Homologous recombination is required for the formation of chromatin bridges but not of UFBs.** (A) HR promotes the formation of chromatin bridges. Dpb11-YFP bridges were counted in wild-type (ML533) and in *sgs1*Δ (SMG223-2C), *rad51*Δ (VS16-3C), *rad52*Δ (VS19-5A), and *sgs1*Δ *rad51*Δ (VS26-15A) cells and scored for Hoechst staining before and after treatment with 0.03% MMS for 70 min. (B) MMS-induced Dpb11 bridges are HR independent. Dpb11-YFP bridges were counted in wild-type (ML533) and in *rad51*Δ (VS16-3C), *rad54*Δ (VS17-1C), and *rad52*Δ (VS19-5A) cells at different time points after addition of 0.03% MMS. (C) Rad51 overexpression induces chromatin bridges. Cells expressing Dpb11-YFP (ML533) were transformed with plasmids for galactose-induced expression of wild-type *RAD51* (pYES-GAL-*RAD51*), a catalytically inactive *rad51-K191R* (pYES-GAL-*rad51-K191R*), or the empty vector (pYES). Cells were grown in SC-Leu containing 2% raffinose and inspected by microscopy after induction with 2% galactose for 1 h and Hoechst staining. (D) Dpb11 suppresses the formation of chromatin bridges by HR. Wild-type *RAD54* (ML628) and *rad54*Δ mutant (VS17-1C) cells were grown 12 h with or without 20 µg/ml doxycycline to repress Dpb11-YFP expression from the *Tet-Off* (*tetO*$_2$) promoter and stained with Hoechst before imaging. Error bars represent 95% confidence intervals. (E) Dpb11 suppresses the formation of Hoechst-positive Rfa1 anaphase bridges. Wild-type (SMG216-10A) cells coexpressing Dpb11-YFP under the control of the *Tet-off* promoter and Rfa1-CFP were grown in the absence or presence of 20 µg/ml doxycycline (Dox) for 12 h to repress expression of Dpb11-YFP and stained with Hoechst before imaging.

Upon repression of *DPB11* expression below the level of detection by fluorescence microscopy, we observed a dramatic increase in the frequency of chromatin bridges. The observed increase in chromatin bridges could reflect either a direct role of Dpb11 in suppressing or resolving chromatin bridges or a defect in DNA replication caused by the low abundance of Dpb11. The observed increase in chromatin bridges depends on HR (Fig. 4 D), which is consistent with the hyper-recombinant phenotype of some *dpb11* mutants (Germann et al., 2011). To determine the frequency of Hoechst-negative anaphase bridges upon Dpb11 repression, we repeated the experiment in a strain expressing Rfa1-CFP as a marker for anaphase bridges. The analysis of this strain confirms that Hoechst-positive bridges accumulate upon Dpb11 depletion, whereas the frequency of Rfa1-marked Hoechst-negative UFBs remains unchanged (Fig. 4 E). In conclusion, we find that Dpb11-marked UFBs are induced by DNA replication stress in a predominantly recombination-independent manner, whereas recombination promotes the formation of Hoechst-positive chromatin bridges.

Dpb11 ultrafine anaphase bridges activate the NoCut cell cycle delay

The delay in nuclear division observed in cells with a Dpb11 anaphase bridge suggests that a checkpoint may be operating

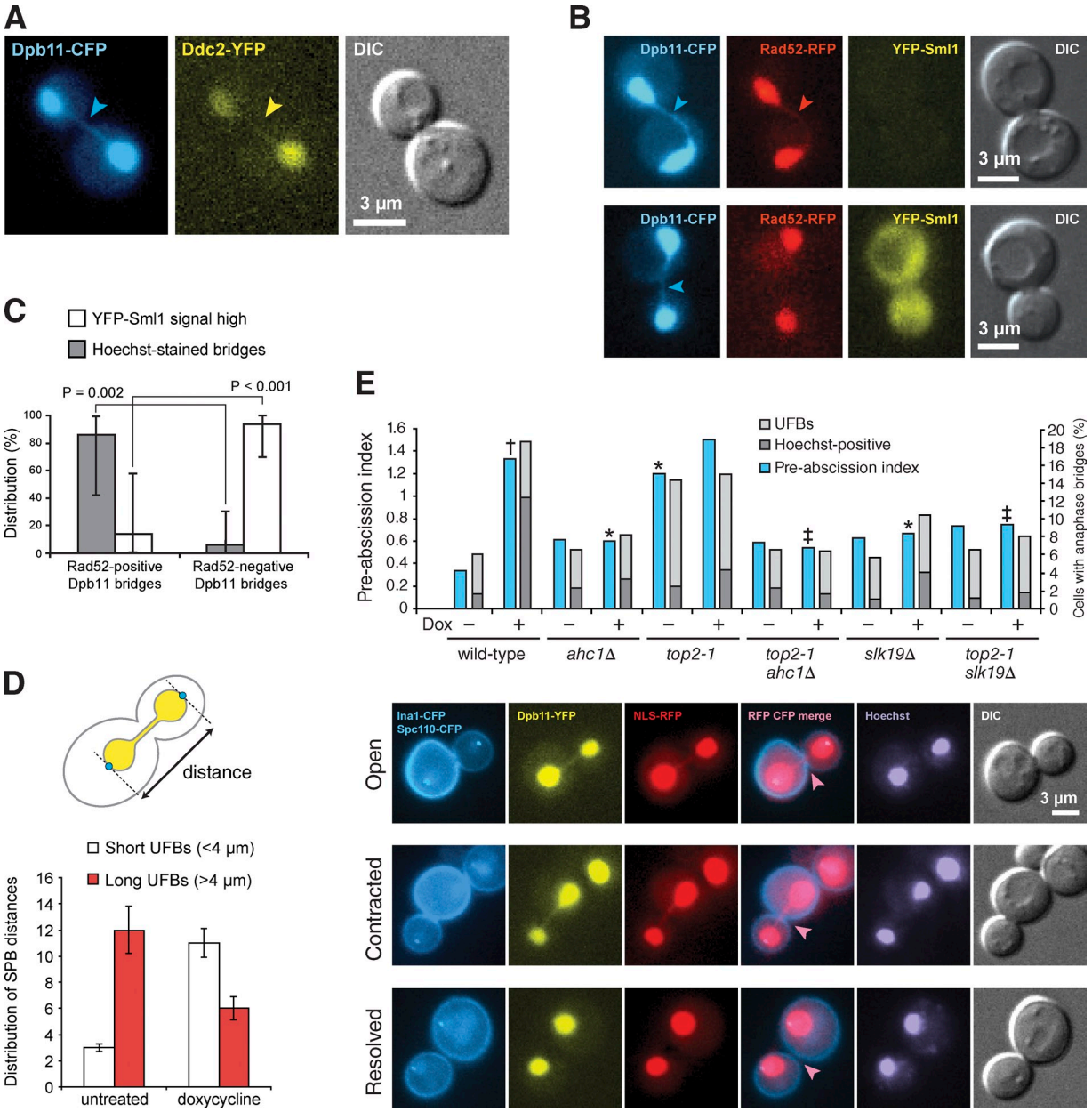

Figure 5. **Chromatin bridges but not UFBs are sensed by the DNA damage checkpoint.** (A) Ddc2 binds to DNA in anaphase bridges. Cells (VS34-1A) coexpressing Ddc2-YFP and Dpb11-CFP were analyzed. (B) Sml1 levels decrease in response to Rad52-bound chromatin bridges. Cells (SMG260-7C) expressing YFP-Sml1, Dpb11-CFP, and Rad52-RFP were analyzed as in A. (C) Chromatin bridges but not UFBs activate the DNA damage response. Hoechst staining and YFP-Sml1 levels were quantified in cells from B with Rad52-positive and Rad52-negative Dpb11 bridges. (D) Dpb11 stabilizes long UFBs. Cells (ML734-9B) coexpressing RFP-NLS, Ina1-CFP, and Spc110-CFP were grown overnight with or without 20 µg/ml doxycycline to repress Dpb11-YFP expression from the *Tet-Off* (*tetO*$_2$) promoter and imaged after Hoechst staining. The length of UFBs (Hoechst-negative RFP bridges; distance between SPBs) was measured in 20 cells for each condition. Error bars represent 95% confidence intervals. (E) The NoCut checkpoint senses Dpb11 bridges. Wild-type (ML734-9B), *ahc1*Δ (ML737-3C), *top2-1* (ML734-11D), *ahc1*Δ *top2-1* (ML737-11A), *slk19*Δ (ML735-1C), and *slk19*Δ *top2-1* (ML735-13A) cells expressing Dpb11-YFP, NLS-RFP, Spc110-CFP, and the plasma membrane marked by Ina1-CFP were grown overnight with or without 20 µg/ml doxycycline (Dox) to repress Dpb11 expression and imaged after Hoechst staining. The abscission index was calculated as the ratio of cells with contracted versus resolved plasma membrane as described previously (Mendoza et al., 2009). The NLS-RFP marker was used to estimate the frequency of UFBs in the Dpb11-depleted cells. For each condition, two independent experiments were performed to examine abscission in 30–78 anaphase cells. *, †, and ‡ indicate significant difference from wild-type, untreated, and *top2-1*, respectively ($P < 0.05$, χ^2 test).

(Fig. 2 F). We decided to test if Dpb11 is required for this checkpoint and if the delay is signaled through stimulation of Mec1 kinase activity (Mordes et al., 2008; Pfander and Diffley, 2011). We therefore first examined the recruitment of Ddc2 to Dpb11 bridges as a proxy for the Ddc2–Mec1 complex. Similar to Dpb11, Ddc2 is recruited to UFBs (Fig. 5 A). Next, we assessed DNA damage checkpoint activation in cells with Dpb11 anaphase bridges by monitoring Sml1 protein levels. In response to DNA damage, Sml1 is subject to Mec1-dependent phosphorylation and subsequent ubiquitylation and degradation by the proteasome (Andreson et al., 2010). Surprisingly, the majority of cells with Rad52- and Hoechst-negative Dpb11 bridges exhibit

Table 1. **Effect of Dpb11 depletion on mitotic *leu2* heteroallelic recombination**

Genotype	Strain	Treatment	Heteroallelic recombination	
			Rate[a] × 10^{-6}	Fold change[b]
Wild type	ML412	–	1.3 ± 0.3	1
Wild type	ML412	dox	1.1 ± 0.3	0.9
$tetO_2$-DPB11	ML767	–	1.3 ± 0.3	1.0
$tetO_2$-DPB11	ML767	dox	2.5 ± 0.5	2.0
ahc1Δ	ML762	–	1.7 ± 0.4	1.3
ahc1Δ	ML762	dox	1.8 ± 0.5	1.4
ahc1Δ $tetO_2$-DPB11	ML768	–	1.9 ± 0.4	1.5
ahc1Δ $tetO_2$-DPB11	ML768	dox	4.1 ± 0.8	3.2

[a]Recombination rate (events per cell per generation) is presented as the mean ± SD.
[b]Relative to the wild type without doxycycline.

high levels of Sml1, indicating that a bona fide DNA damage checkpoint has not been activated. In contrast, Rad52- and Hoechst-positive Dpb11 bridges activate the DNA damage checkpoint, leading to Sml1 degradation (Fig. 5, B and C). Although only chromatin bridges activate the DNA damage checkpoint, both types of anaphase bridges delay abscission (Fig. 2 F and Fig. 5 E; Mendoza et al., 2009). To test directly whether Dpb11 is required to delay abscission, we monitored abscission after shutting off expression of Dpb11 by addition of doxycycline. Abscission was assessed using endogenously tagged Ina1 (*YLR413W*, indicator of abscission 1). Ina1 exhibits plasma membrane localization similar to the PH domain that was originally used to assess abscission (Mendoza et al., 2009; Fig. S3). Reduction in Dpb11 expression leads to an accumulation of chromatin bridges, a shift from long to short anaphase bridges, and delayed abscission, demonstrating that Dpb11 is not required for the NoCut checkpoint (Fig. 5, D and E). In contrast, disruption of the previously described NoCut checkpoint by deletion of *AHC1* or *SLK19* suppressed the accumulation of pre-abscission cells after *DPB11* repression (Fig. 5 E). To test the consequence of premature abscission in the Dpb11-depleted cells, we measured spontaneous recombination between two nonfunctional *leu2* heteroalleles in diploid cells. Whereas *ahc1*Δ or depletion of Dpb11 individually increased interhomologue recombination mildly, the combination of Dpb11 depletion and disruption of the NoCut checkpoint led to a synergistic increase in HR (Table 1).

Because Dpb11 stimulates Mec1 to phosphorylate a number of checkpoint and repair proteins including the Rad53 kinase, we also monitored Dpb11 bridges in *mec1*Δ *sml1*Δ and *rad53*Δ *sml1*Δ DNA damage checkpoint–defective strains. Interestingly, both mutants exhibit elevated levels of anaphase bridges with *mec1*Δ *sml1*Δ inducing primarily UFBs and *rad53*Δ *sml1*Δ mostly chromatin bridges (Fig. S4), suggesting that Mec1 and Rad53 are also required to suppress the formation of anaphase bridges. In conclusion, Dpb11 ultrafine anaphase bridges do not activate a bona fide DNA damage checkpoint; rather, Dpb11 is required to suppress the formation of chromatin anaphase bridges by HR.

Recruitment of Dpb11/TopBP1 to UFBs is evolutionarily conserved

PICH-covered UFBs have so far only been observed in mammalian cells. To address whether UFBs also exist in the avian DT40 cell line, we tagged the PICH gene with mTurquoise2 (TFP; Goedhart et al., 2012) or YFP at the endogenous locus. As a marker for chromatin, cells were stably transfected with mCherry-tagged human H2B (hH2B-mCherry). By live-cell microscopy, we readily detected PICH-covered bridges connecting the separating chromosome masses in anaphase cells (Fig. 6 A). Notably, the PICH-coated bridges in untreated DT40 cells neither stained with Hoechst nor did they colocalize with the hH2B-mCherry signal, suggesting that they are uncondensed bona fide UFBs (Baumann et al., 2007; Chan et al., 2009).

The vertebrate orthologue of Dpb11 is TopBP1, which was identified as a topoisomerase IIβ–binding protein (Yamane et al., 1997). TopBP1 is required for DNA replication and provides a scaffold for DNA damage checkpoint activation (Mäkiniemi et al., 2001; Lindsey-Boltz and Sancar, 2011). To test the evolutionary conservation of the role of Dpb11 during anaphase, we examined DT40 cells expressing TopBP1-YFP from the endogenous locus. Time-lapse analysis showed that TopBP1 and PICH indeed colocalize at some chromatin-free UFBs from early anaphase until cytokinesis. However, a subset of PICH UFBs are not or only transiently bound by TopBP1 (Fig. 6 B). As mitosis progresses, PICH is the first to dissociate from the UFBs, forming temporary sister foci at the UFB termini (Fig. 6, B and C; and Video 1). In human cells, PICH-bound UFBs and chromatin bridges can be induced by the polymerase α inhibitor aphidicolin (APH) or the topoisomerase II inhibitor ICRF-193 (Baumann et al., 2007; Chan et al., 2009). We find that ICRF-193 also induces PICH-covered UFBs as well as chromatin bridges in DT40, whereas APH treatment specifically stimulates the formation of chromatin bridges and colocalizing PICH and TopBP1 bridges (Fig. 7 A). In untreated anaphase cells, TopBP1 localizes to bridge-like structures in 78% of anaphase cells (Fig. 7 A). About 27% of the TopBP1-bound bridges colocalize with PICH UFBs, increasing to 41% after APH treatment, while being largely unaffected by ICRF-193 treatment (Fig. 7 A). The PICH-negative TopBP1 bridges could represent TopBP1 localization at the midbody (Reini et al., 2004).

Interestingly, TopBP1 localization appears to be restricted to a smaller region of the PICH-coated UFBs, at which TopBP1 remains even after dissociation of PICH in late telophase (Fig. 6, B and C). To address whether this region contains single-stranded DNA, we followed the localization of RPA relative to

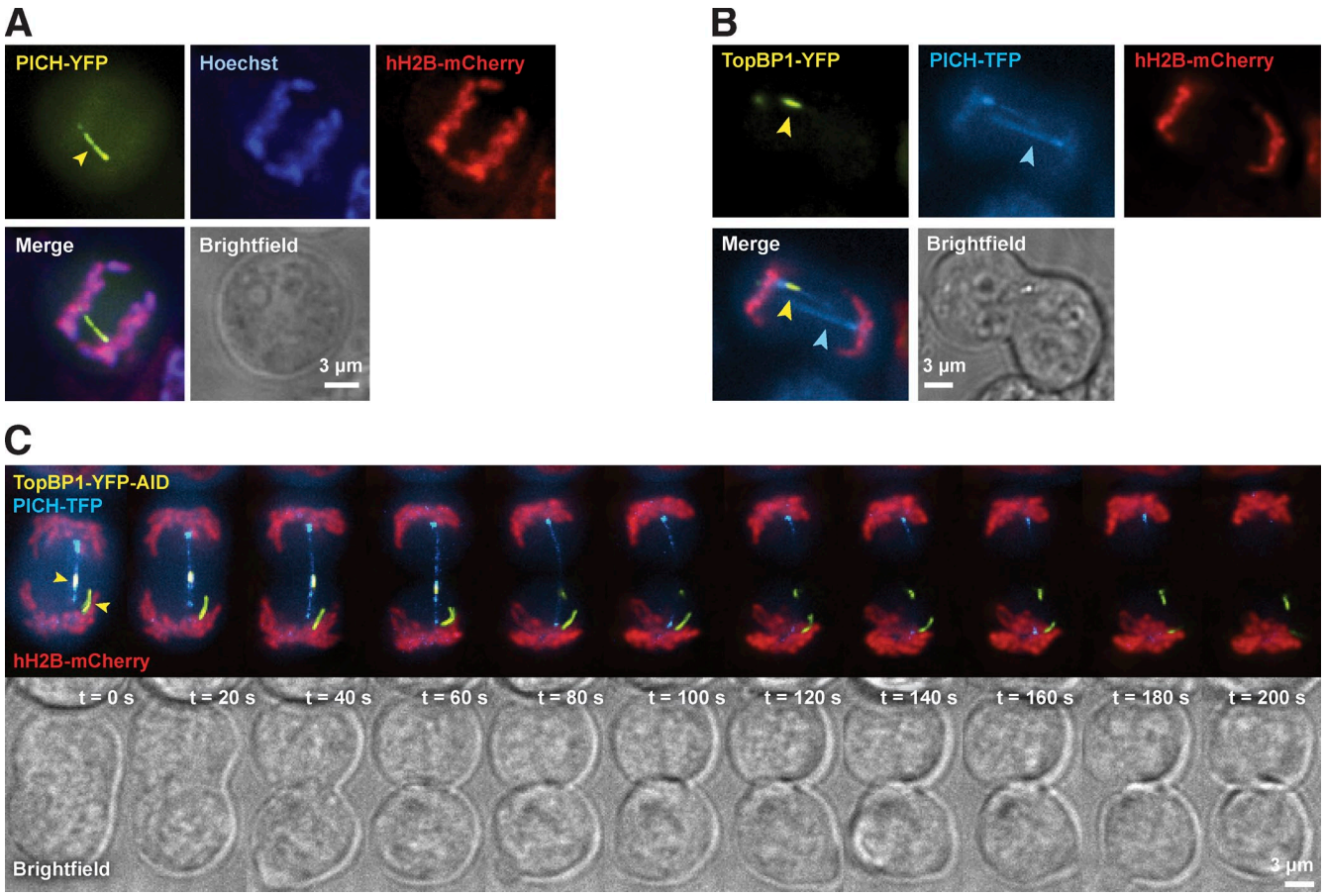

Figure 6. **Recruitment of TopBP1 to anaphase bridges is evolutionarily conserved.** (A) PICH coats hH2B- and Hoechst-negative UFBs in DT40 cells. Cells (RTP82) expressing PICH-YFP from its endogenous promoter and randomly integrated hH2B-mCherry were stained with Hoechst. Arrowhead indicates a UFB. (B) PICH and TopBP1 colocalize at a subset of UFBs. Cells (RTP149) express TopBP1-YFP and PICH-TFP from their endogenous promoters and hH2B-mCherry. Yellow arrowhead indicates the site of PICH and TopBP1 colocalization at a UFB. Blue arrowhead indicates a PICH-coated UFB without TopBP1. (C) PICH dissociates from UFBs before TopBP1 to form transient sister foci at the termini of the UFB as the cell progresses through anaphase and telophase. Representative time-lapse image sequence of cells (RTP151) expressing TopBP1-YFP-AID and PICH-TFP from their endogenous promoters and randomly integrated OsTIR1 and hH2B-mCherry. Arrowheads indicate TopBP1 structures.

TopBP1 (Fig. 7 B and Video 2). Interestingly, 24% and 45% of TopBP1 bridges colocalize with RPA after APH or ICRF-193 treatment, respectively, whereas RPA and TopBP1 rarely (1%) colocalize in spontaneous TopBP1 bridges (Fig. 7 C). Importantly, 86% and 83% of the RPA foci observed between the separating chromosomes colocalize with TopBP1 after APH or ICRF-193 treatment, respectively. In conclusion, avian TopBP1 colocalizes with PICH UFBs, and this colocalization is increased in response to replication stress. Moreover, we find that a subset of TopBP1 bridges may contain single-stranded DNA.

TopBP1 depletion causes accumulation of chromatin bridges in anaphase

To determine the impact of TopBP1 on anaphase bridges, we constructed a cell line where all three alleles of TopBP1 are tagged with YFP followed by an auxin-inducible degron (AID), TopBP1-YFP-AID (Nishimura et al., 2009). When expressing the F-box transport inhibitor response protein 1 from *Oryza sativa* (OsTIR1) in these cells, addition of auxin (IAA) promotes interaction between OsTIR and TopBP1-YFP-AID, resulting in polyubiquitylation of the AID degron and targeting of TopBP1-YFP-AID for degradation by the proteasome (Nishimura et al., 2009). Depletion of TopBP1 by addition of IAA 30 min before anaphase led to an induction of chromatin bridges and a decreased frequency of UFBs during anaphase (Fig. 7 D). Moreover, depletion of TopBP1 completely inhibited the formation of long PICH-coated UFBs (Fig. 7 F). In fact, PICH UFBs that extend beyond 5 µm are always (98%) bound by TopBP1 (Fig. S5 A). This effect does not appear to be caused by replication stress because APH treatment does not affect the length distribution of PICH-coated bridges (Fig. 7 G), nor can we detect any DNA synthesis during the last 30 min before anaphase entry as based on EdU incorporation, indicating that bulk DNA replication is completed at this stage (Fig. S5, B and C).

To test whether the effect of TopBP1 depletion on DNA bridges is due to its role as an activator of ATR (Kumagai et al., 2006), we treated cells with an ATR inhibitor (ATRi) before anaphase onset (Toledo et al., 2011). Similar to depletion of TopBP1-YFP-AID, treatment with ATRi increased chromatin bridges (Fig. 7 E). However, contrary to depletion of TopBP1-YFP-AID, treatment with ATRi increased the amount of TopBP1-bound UFBs and induced a shift from short to long PICH-coated

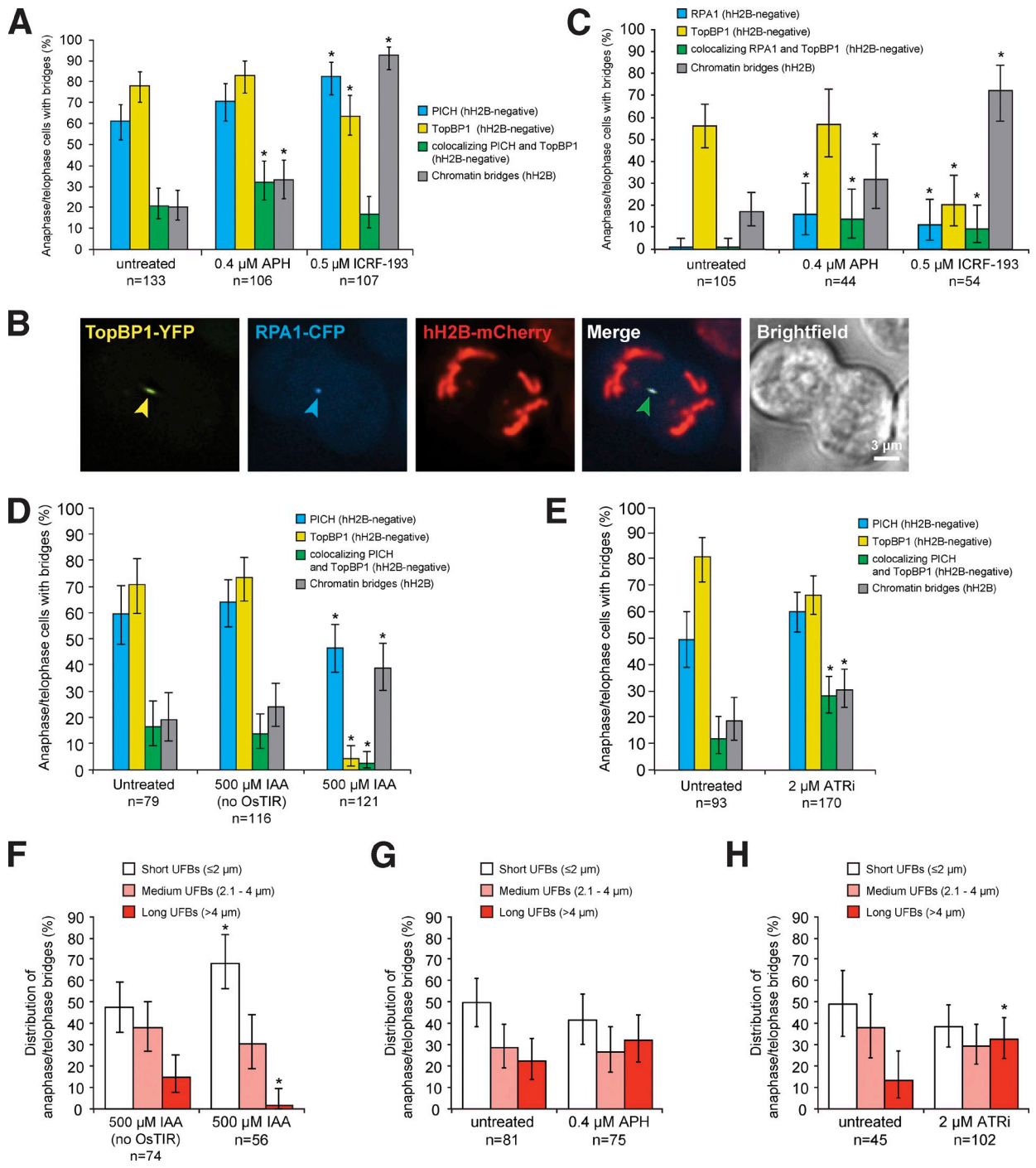

Figure 7. **TopBP1 is required for timely resolution of anaphase bridges.** In all experiments, quantification was performed on the basis of time-lapse microscopy with an imaging frequency of 2 min for 30 min. Exponentially growing cells were monitored from anaphase through telophase, and bridges were scored. The maximum number of bridges visible at one time point was noted as representative for the entire mitosis of a given cell. Asterisk indicates significant differences from the untreated ($P < 0.05$); error bars represent 95% confidence intervals. The number of cells analyzed is indicated (n). (A) TopBP1 and PICH colocalizing UFBs are induced by DNA replication stress but not topological stress. Cells expressing TopBP1-YFP-AID, PICH-TFP, OsTIR, and hH2B-mCherry (RTP151) were treated with 0.4 μM APH for 24 h, 0.5 μM ICRF-193 for 30 min, or 0.0125% DMSO (vol/vol, untreated) for 24 h before imaging. (B) A subset of TopBP1 bridges colocalizes with RPA. Cells (RTP156) express TopBP1-YFP, RPA1-CFP, and hH2B-mCherry. Yellow, blue, and green arrowheads indicate TopBP1, RPA1, and colocalizing bridges, respectively. (C) Colocalization of TopBP1 and RPA bridges is induced by both DNA replication stress and topological stress. Cells expressing TopBP1-YFP, RPA-CFP, and hH2B-mCherry (RTP156) were treated with 0.4 μM APH for 24 h, 0.5 μM ICRF-193 for 30 min, or 0.0125% DMSO (vol/vol, untreated) for 24 h before imaging. (D) Depletion of TopBP1 leads to a reduction of UFBs and induction of chromatin bridges. Cells expressing TopBP1-YFP-AID, PICH-TFP, and hH2B-mCherry with OsTIR present (RTP151) or absent (RTP177) were treated with 500 μM IAA or 0.2% ethanol (vol/vol, untreated) for 30 min before imaging. After incubation with IAA for 30 min, the level of TopBP1-YFP-AID fluorescence had decreased below detection in the majority of cells. (E) ATR inhibition induces chromatin bridges and colocalizing PICH- and TopBP1-coated UFBs. Cells expressing TopBP1-YFP-AID, PICH-TFP, OsTIR, and hH2B-mCherry (RTP151) were treated with 2 μM ATRi or 0.2% DMSO (vol/vol, untreated) for 30 min before imaging. (F–H) TopBP1 depletion, replication stress, and ATR inhibition affect the length of PICH UFBs. The length distribution of UFBs was quantified in anaphase/telophase cells from panels D (IAA), A (APH), and E (ATRi).

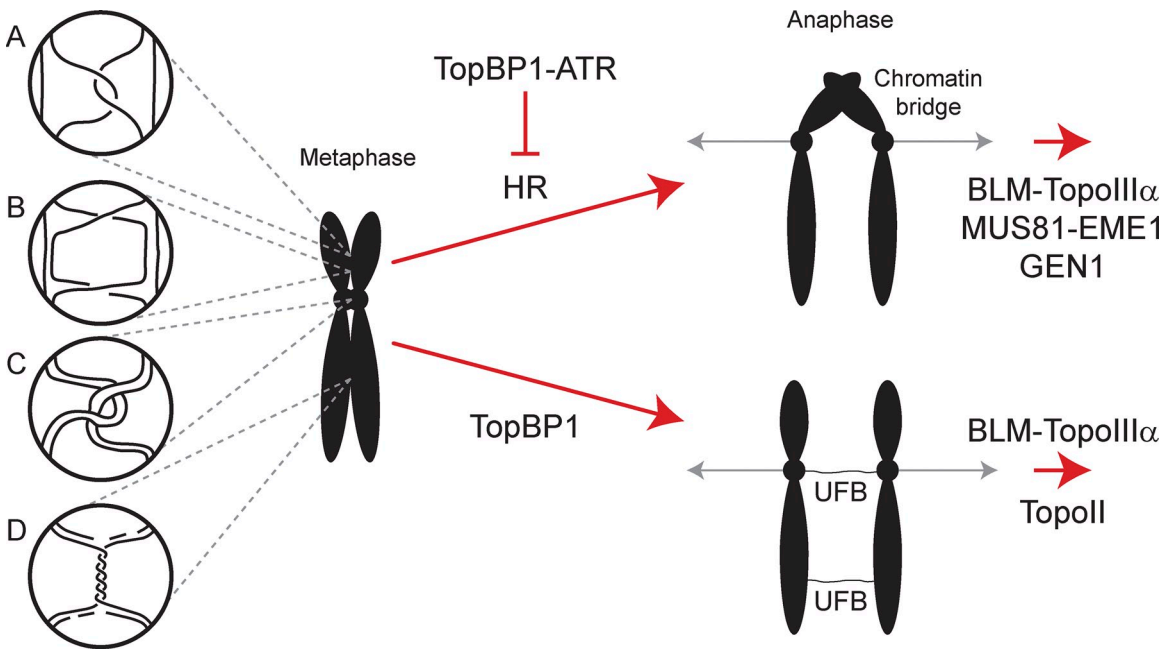

Figure 8. **Model for Dpb11/TopBP1 function at anaphase bridges.** During metaphase, the sister chromatids may be interlinked by hemicatenanes (A), Holliday junctions (B), catenanes (C), and unreplicated regions or termination zones (D). The hemicatenanes and unreplicated regions contain single-stranded DNA, which may act as a substrate to initiate homologous recombination (HR), leading to the formation of chromosomes connected by Holliday junctions. TopBP1-ATR inhibits recombination at replication forks and BLM-TopoIIIα promotes the nonrecombinogenic dissolution of hemicatenanes. Double-Holliday junctions can also be resolved by MUS81-EME1 or GEN1. During anaphase any remaining catenanes must be resolved by TopoII to prevent chromosome nondisjunction. The interaction of TopoII with TopBP1 may aid this process.

UFBs (Fig. 7 H). These data indicate that TopBP1 suppresses the formation of chromatin bridges to ensure proper segregation of chromosomes by a mechanism that only partially overlaps with its role as an ATR activator.

Discussion

In this study, we establish budding yeast and the avian DT40 cell line as model systems for studying DNA anaphase bridges. In both yeast and DT40 cells we find that when Dpb11/TopBP1 localizes to UFBs, it facilitates their elongation or stability while it suppresses the formation of chromatin bridges. In yeast, Dpb11 UFBs do not activate a bona fide DNA damage checkpoint as measured by Sml1 degradation; instead, anaphase bridges delay abscission by the NoCut checkpoint, independently of Dpb11. Accordingly, simultaneous disruption of the NoCut checkpoint and depletion of Dpb11 led to a synergistic increase in genome instability as measured by interhomologue recombination. In *Schizosaccharomyces pombe*, which does not appear to have a NoCut checkpoint, the Dpb11/TopBP1 orthologue Cut5 was identified along with *top2* mutants for their *cut* phenotype (Hirano et al., 1986), indicating that Cut5 plays a similar role in *S. pombe* in suppressing or resolving anaphase bridges.

Using the budding yeast and DT40 model systems, we tested the proposed sources of anaphase bridges and their putative mechanisms of resolution (Fig. 8): four different DNA structures have been suggested to form anaphase bridges: (1) hemicatenanes arising during DNA replication, (2) catenanes, (3) unreplicated regions of the genome or replication termination zones, and (4) single- and double-Holliday junctions arising from HR.

In *Saccharomyces cerevisiae*, hemicatenanes form during DNA replication in a Rad52-independent manner (Lopes et al., 2003; Wellinger et al., 2003) and have been proposed to be resolved by the Sgs1–Top3–Rmi1 (BLM-TopoIIIα–RMI1-RMI2) complex (Wu and Hickson, 2003). Our finding that the frequency of Dpb11 anaphase bridges dramatically increases in an *sgs1*Δ mutant is indicative of hemicatenes constituting a source for anaphase bridges in otherwise unchallenged cells. The anaphase bridges that accumulate in *sgs1*Δ cells are Hoechst positive and dependent on HR for their formation, which is consistent with overexpression of Rad51 leading to chromatin bridges, and with the report that hemicatenes are converted by Rad51 to recombination intermediates in the absence of Sgs1 (Liberi et al., 2005). Likewise, in BLM-deficient human cells elevated levels of both chromatin bridges and lagging chromosomes as well as PICH bridges are observed (Chan et al., 2007).

Catenanes are formed by the noncovalent intertwining of sister chromatids. The primary decatenating activity of the cell is provided by topoisomerase II. To assess the contribution of catenanes in the formation of anaphase bridges, we took advantage of a temperature-sensitive *top2-1* mutant in yeast (Brill et al., 1987) or the topoisomerase II inhibitor ICRF-193 in DT40 cells. In yeast, mutation of *TOP2* leads to an accumulation of UFBs at the semipermissive temperature and to an increase of both UFBs and chromatin bridges at the restrictive temperature. Similarly, ICRF-193 induces both chromatin and PICH UFBs in DT40 cells, which is consistent with results from human cells, where ICRF-159 was reported to induce BLM bridges in a dose-dependent manner (Chan et al., 2007). Thus, our data indicate that sister chromatid catenanes are a source of UFBs in both yeast and DT40 cells.

DNA replication stress induced by MMS or HU in *S. cerevisiae* or by APH in DT40 cells also leads to UFBs, as previously reported for human cells and *S. pombe* (Chan et al., 2009; Sofueva et al., 2011). Moreover, MMS treatment and the *top2-1* mutation were additive for induction of UFBs, indicating that replication and topological stress independently lead to these structures.

The majority of chromatin bridges that we observe in *S. cerevisiae* require *RAD51*, *RAD52*, and *RAD54*, indicating that these structures form through HR. This is further supported by the observation that chromatin bridges are bound by Rad52 and trigger degradation of Sml1, indicating that these structures lead to DNA damage signaling. Moreover, chromatin bridges can be induced by overexpression of Rad51 but not by catalytically inactive Rad51 (*rad51-K191A*). Thus, our work proposes that HR intermediates are a substantial source of chromatin bridges. In line with this, a number of recent articles report that Holliday junction resolvases including MUS81-EME1 and SLX1-SLX4 act in mitosis to preserve genome stability (Matos et al., 2013; Naim et al., 2013; Szakal and Branzei, 2013; Wyatt et al., 2013; Ying et al., 2013). The notion that UFBs are formed independently of HR is supported by RAD51 knockdown in human cells (Chan et al., 2009; Lahkim Bennani-Belhaj et al., 2010). However, the latter study also reported an increase in BLM-associated chromatin bridges upon knockdown of RAD51, which in the light of our data from yeast could reflect stalled HR due to residual RAD51 levels allowing HR to initiate but not supporting its completion.

Based on these results we propose two mutually nonexclusive roles for Dpb11/TopBP1 at anaphase bridges: (1) suppressing the formation of chromatin bridges and (2) facilitating chromosome segregation through the extension and stabilization of UFBs. Concerning the first point, it has been shown that Dpb11/TopBP1 stimulates Mec1/ATR kinase activity, which in turn regulates HR at replication structures (Lisby et al., 2004; Meister et al., 2005; Kumagai et al., 2006; Mordes et al., 2008; Chanoux et al., 2009; Pfander and Diffley, 2011), pointing to a model where Dpb11/TopBP1 suppresses the formation of anaphase bridges by facilitating the Mec1/ATR-dependent replication checkpoint, thus inhibiting fork collapse and HR (Fig. 8). This is supported by our finding that direct inhibition of the ATR kinase in DT40 cells leads to an accumulation of chromatin bridges, which partially phenocopies auxin-mediated depletion of TopBP1. We have observed a similar increase in the frequency of chromatin bridges in a yeast *rad53*Δ *sml1*Δ mutant, whereas a *mec1*Δ *sml1*Δ mutant primarily exhibited an increase in UFBs. The difference between the *rad53*Δ and *mec1*Δ mutant phenotypes could be rationalized by the reported Mec1-independent activities of Rad53 (Clerici et al., 2001; Schramke et al., 2001; Corda et al., 2005). Concerning the second point, stabilizing bridges to help chromosome segregation, the opposing effects of TopBP1 depletion and ATR inhibition on the length distribution of PICH-coated UFBs in DT40 cells indicate that TopBP1 also has a more direct effect on ultrafine bridges, in addition to activating ATR. Dpb11/TopBP1 remains associated with UFBs until late anaphase and apparently facilitates the extension/stability of long UFBs because PICH UFBs rarely extend beyond 5 µm without being bound by TopBP1. This may be related to the interaction of TopBP1 with topoisomerase IIβ (Yamane et al., 1997), which could facilitate the recruitment of topoisomerase IIβ to sites of catenation allowing for progressive disentangling of intertwined sister chromatids. On the other hand, topoisomerase IIα is believed to perform the bulk of decatenation in human cells and depletion of topoisomerase IIα leads to shortening of the metaphase interkinetochore distance and abnormal persistence of PICH-coated anaphase bridges (Porter and Farr, 2004; Spence et al., 2007; Wang et al., 2010). It is not known whether Dpb11 and Top2 interact in yeast, but their frequent colocalization on UFBs could suggest a potential interaction.

The relationship between UFBs and chromatin bridges remains an important open question. However, in the hundreds of anaphase time-lapse microscopy sequences that we have acquired, we have never observed a chromatin bridge turning into a UFB or vice versa. Hence, the determination for a potential initial DNA structure to develop into a chromatin bridge or a UFB appears to be made before anaphase onset. Moreover, several mutants and genotoxic agents induce both kinds of anaphase bridges, suggesting that processing of the initiating DNA structure and its timing relative to, for example, chromosome condensation, may determine whether an anaphase bridge is chromatinized or not.

Materials and methods

Yeast strains and cell culture

Media and standard genetic techniques to manipulate yeast strains were described previously (Sherman, 2002). All yeast strains used in this study are *RAD5* derivatives of W303 (Table S1). DT40 cell culture and transfection were done as described previously (Buerstedde and Takeda, 1991). DT40 cell lines used in this study are listed in Table S2.

Construction of yeast plasmids and fluorescent fusion proteins

All plasmids are described in Table S3. Oligonucleotide sequences are available upon request. Unless otherwise noted, fluorescent fusion proteins were constructed as described previously (Lisby et al., 2004; Silva et al., 2012). Plasmids pML96 and pML104 for integrating the NLS-RFP fusion protein into the *ura3-1* and *his3-11,15* loci, respectively, were constructed by first amplifying yEmRFP from pNEB30 using KpnI and EcoRI-adapted primers NLSyEmRFP-F and NLSyEmRFP-R, respectively, that adds the SV40-NLS (PKKKRKVEDP) to the N-terminal end of yEmRFP (Silva et al., 2012). The KpnI–EcoRI-digested PCR product was cloned into KpnI–EcoRI-linearized pGAD-C2 behind the *ADH1* promoter (James et al., 1996). Next, the ADH1-NLS-yEmRFP expression cassette was subcloned into the SphI site of the *URA3*-integrative vector YIp5 (Struhl et al., 1979) to yield pML96. To generate a *HIS3*-based derivative of pML96, a NaeI–AfeI restriction fragment containing *HIS3* was subcloned from pRS413 (Sikorski and Hieter, 1989) into NruI–BsaBI-digested pML96 to replace *URA3* and produce pML104. For integration into the *ura3-1* and *his3-11,15* loci, pML96 and pML104 were linearized with ApaI and BsmI, respectively, before transformation into ML8-9A.

Generation of DT40 knock-in constructs

DT40 genes were endogenously tagged at their 3′-termini. The 3′ and 5′ arms of the TopBP1-YFP-AID knock-in construct were subcloned from pVHO3. To generate 3′ and 5′ arms for the PICH-YFP/TFP knock-in constructs, flanking regions of homology immediately 5′ and 3′ of the PICH stop codon were amplified from DT40 genomic DNA. The AID, YFP, and TFP tags were amplified from pMK43, pEYFP-C1, and pmTurquoise2-N1, respectively. Primer pairs were designed to facilitate directional cloning. The amplified PCR products were cloned into the pCR2.1-TOPO vector (Invitrogen) and coding regions sequenced. As a sequence reference for the 3′ and 5′ arms of the PICH knock-in constructs, the genomic DNA sequence of *Gallus gallus* (DT40) was obtained from the National Center for Biotechnology Information (Gene ID: 422135). The BSR, NEO, and

PURO cassettes were subcloned from pLOX-BSR, pLOX-NEO, and pLOX-PURO, respectively.

For assembly of the PICH-TFP/YFP knock-in constructs (pRTP6, pRTP9, and pRTP17), the 3′-arm, a BSR/PAC cassette, the 5′-arm, and the YFP/TFP tag were individually subcloned into pBlueScript SK+ in the listed order using restriction sites XbaI–NotI, BamHI, KpnI–SalI, and SalI–EcoRI, respectively.

For assembly of the TopBP1-YFP-AID knock-in constructs (pRTP14, pRTP15, and pRTP16), the YFP tag, the AID tag, the 3′-arm, and a BSR/NEO/PAC cassette were individually subcloned into pVHO3 in the listed order using restriction sites XbaI–NotI, BamHI–BglII, BglII–NotI, and BamHI, respectively.

For assembly of hH2B-mCherry under expression control of chicken β-actin promoter (pRTP23), hH2B-mCherry was subcloned from pH2B_mCherry_IRES_neo3 into pExpress using the restriction site HindIII. The β-actin promoter and hH2B-mCherry were subsequently subcloned into pLOX-PURO using restriction site SpeI.

The targeting constructs were linearized with NotI before transfection. Transfectants harboring the *PAC*, *NEO*, and *BSR* resistance genes were selected in the presence of 0.5 µg/ml puromycin, 2 mg/ml G418, and 20 µg/ml blasticidin, respectively. The resistance cassettes were loxed as described previously (Arakawa et al., 2001). In brief, cell lines were transiently transfected with cDNA encoding the Cre recombinase and subsequently dilution cloned to obtain single colonies. Loss of selection markers was tested by treating the resulting cell lines with puromycin, G418, or blasticidin. Integration of the YFP/TFP/YFP-AID tags at the correct genomic location was confirmed by PCR analysis of genomic DNA.

Microscopy and immunofluorescence

Yeast cells were grown in synthetic complete (SC) medium supplemented with 100 µg/ml adenine (SC+Ade) and processed for fluorescence microscopy as described previously (Eckert-Boulet et al., 2011). For staining of DNA in live yeast cells, 10 µg/ml of DAPI or 5 µg/ml of Hoechst 33258 (B2883; Sigma-Aldrich) was added to the culture 10–15 min before microscopy and washed out with fresh medium immediately before microscopy and imaged at 25°C or 37°C as indicated. Fluorophores used in yeast were CFP (clone W7; Heim and Tsien, 1996), YFP (clone 10C; Ormö et al., 1996), and rRFP (clone yEmRFP; Keppler-Ross et al., 2008).

DT40 cells were imaged at 39°C in RPMI 1640 medium GlutaMAX (Gibco) supplemented with 2% chicken serum (Gibco), 8% fetal bovine serum (Gibco), 2 mM L-glutamine (Gibco), 55 µM β-mercaptoethanol, 50 U/ml penicillin, and 50 µg/ml streptomycin, and mounted on µ-slides before imaging (Ibidi). For staining of DNA in live DT40 cells, 5 µg/ml of Hoechst 33342 (Sigma-Aldrich) was added to the culture 30 min before microscopy. Where indicated, 500 µM indole-3-acetic acid (IAA; Sigma-Aldrich) or 2 µM ATRi was added for the indicated amount of time before imaging.

Fluorophores were visualized on a microscope (AxioImager Z1; Carl Zeiss) equipped with a 100× objective lens (Plan Apochromat, NA 1.4; Carl Zeiss), a cooled CCD camera (Orca-ER; Hamamatsu Photonics), differential interference contrast, and an illumination source (HXP120C; Carl Zeiss); or on a microscope (DeltaVision Elite; Applied Precision) equipped with a 100× objective lens (U-PLAN S-APO, NA 1.4; Olympus), a cooled EMCCD camera (Evolve 512; Photometrics), and a solid-state illumination source (Insight; Applied Precision, Inc). Images were acquired using Volocity (PerkinElmer) or softWoRx (Applied Precision) software. Images were processed and quantitative measurements of fluorescence intensities were performed with Volocity software (PerkinElmer). Images were pseudocolored according to the approximate emission wavelength of the fluorophores. Distances were calculated in 3D based on the X, Y, and Z coordinates obtained from Z-stacks of images in Volocity. Fluorophores used in DT40 were enhanced CFP (ECFP; Takara Bio Inc.), TFP (clone pmTurquoise2-N1; Goedhart et al., 2010), enhanced YFP (EYFP; Takara Bio Inc.), and mCherry (Shaner et al., 2004).

EdU incorporation

For EdU incorporation in yeast, cells were grown to exponential phase at 25°C in SC+Ade medium before addition of 20 µM EdU and continued incubation in an orbital shaker for 3 h. Cells were then fixed in 3.7% PFA for 1 h, and stained with 5 µg/ml Hoechst 33258 (B2883; Sigma-Aldrich). EdU was detected as described in the Click-iT EdU Alexa Fluor 594 imaging kit manual (Invitrogen).

For EdU incorporation in DT40, cells were treated with 10 µM EdU and either 500 µM IAA or 0.2% ethanol (vol/vol, untreated) for 30 min. Cells were washed and resuspended in PBS, and allowed to adhere to poly-L-lysine–coated coverslips for 10 min. Cell fixation, permeabilization, and EdU detection was performed as described in the Click-iT EdU Alexa Fluor 594 imaging kit manual.

Recombination assay

Interchromosomal mitotic recombination between *leu2* heteroalleles was measured by growing diploid strains at 25°C overnight in 3 ml SC+Ade medium before plating on SC with or without leucine (Smith and Rothstein, 1995). Colony-forming units were counted after incubation at 25°C for 3 d. The median frequency for 7–11 trials was used to determine the recombination rate by the method of the median. In brief, the median frequency is divided by the factor r_0/m to obtain the recombination rate, where m is the mean number of Leu^+ recombination events, which have occurred in the culture, and r_0 is the number of events in the trial with the median frequency. The factor r_0/m was estimated by Lea and Coulson (1949) and the standard deviation was calculated as $m \cdot \mathrm{sqrt}((12.7/(2.24 + \ln(m))^2)/N)$, where N is the number of trials (Lea and Coulson, 1949).

Statistical methods

For microscopy experiments, the significance of the differences between cell populations was determined by one-tailed Fisher's exact test. P-values were defined as significant if $P < 0.05$.

Online supplemental material

Fig. S1 shows that Rfa1 binds yeast anaphase DNA bridges. Fig. S2 shows that cells rebud after resolution of anaphase bridges. Fig. S3 shows colocalization of the PH domain and Ina1. Fig. S4 shows that Dpb11 bridges accumulate in *mec1Δ* and *rad53Δ* mutants. Fig. S5 shows EdU incorporation in DT40 and the length distribution of TopBP1/PICH UFBs. Video 1 shows time-lapse microscopy of TopBP1 and PICH. Video 2 shows time-lapse microscopy of TopBP1 and RPA. Table S1 lists the genotype and source of yeast strains used in this study. Table S2 lists the genotype and source of DT40 cell lines used in this study. Table S3 lists plasmids used in this study. Online supplemental material is available at http://www.jcb.org/cgi/content/full/jcb.201305157/DC1.

We thank R. Rothstein and R. Sternglanz for sharing yeast strains; S. Takeda and K.J. Patel for DT40 cell lines; and K. Weis, H. Klein, R. Wellinger, C.S. Sørensen, L.I. Toledo, O.M. Aparicio, R. Benezra, T.W.J. Gadella, and S. Takeda for plasmids and reagents.

This work was supported by The Danish Agency for Science, Technology and Innovation, the Villum Kann Rasmussen Foundation, the Lundbeck Foundation, and the European Research Council (ERC) to M. Lisby; the Deutscher Akademischer Auslandsdienst (DAAD) scholarship and Kræftens Bekæmpelse to S.M. Germann; the DFF to N. Eckert-Boulet; the Villum Kann Rasmussen Foundation to V.H. Oestergaard; the Marie Curie FP7 program to V. Schramke; and the ERC to I. Gallina and R.T. Pedersen.

Submitted: 31 May 2013
Accepted: 25 November 2013

References

Andreson, B.L., A. Gupta, B.P. Georgieva, and R. Rothstein. 2010. The ribonucleotide reductase inhibitor, Sml1, is sequentially phosphorylated, ubiquitylated and degraded in response to DNA damage. *Nucleic Acids Res.* 38:6490–6501. http://dx.doi.org/10.1093/nar/gkq552

Arakawa, H., D. Lodygin, and J.M. Buerstedde. 2001. Mutant loxP vectors for selectable marker recycle and conditional knock-outs. *BMC Biotechnol.* 1:7. http://dx.doi.org/10.1186/1472-6750-1-7

Baumann, C., R. Körner, K. Hofmann, and E.A. Nigg. 2007. PICH, a centromere-associated SNF2 family ATPase, is regulated by Plk1 and required for the spindle checkpoint. *Cell*. 128:101–114. http://dx.doi.org/10.1016/j.cell.2006.11.041

Brill, S.J., S. DiNardo, K. Voelkel-Meiman, and R. Sternglanz. 1987. Need for DNA topoisomerase activity as a swivel for DNA replication for transcription of ribosomal RNA. *Nature*. 326:414–416. http://dx.doi.org/10.1038/326414a0

Buerstedde, J.M., and S. Takeda. 1991. Increased ratio of targeted to random integration after transfection of chicken B cell lines. *Cell*. 67:179–188. http://dx.doi.org/10.1016/0092-8674(91)90581-I

Chan, K.L., and I.D. Hickson. 2009. On the origins of ultra-fine anaphase bridges. *Cell Cycle*. 8:3065–3066. http://dx.doi.org/10.4161/cc.8.19.9513

Chan, K.L., and I.D. Hickson. 2011. New insights into the formation and resolution of ultra-fine anaphase bridges. *Semin. Cell Dev. Biol.* 22:906–912. http://dx.doi.org/10.1016/j.semcdb.2011.07.001

Chan, K.L., P.S. North, and I.D. Hickson. 2007. BLM is required for faithful chromosome segregation and its localization defines a class of ultrafine anaphase bridges. *EMBO J.* 26:3397–3409. http://dx.doi.org/10.1038/sj.emboj.7601777

Chan, K.L., T. Palmai-Pallag, S. Ying, and I.D. Hickson. 2009. Replication stress induces sister-chromatid bridging at fragile site loci in mitosis. *Nat. Cell Biol.* 11:753–760. http://dx.doi.org/10.1038/ncb1882

Chanoux, R.A., B. Yin, K.A. Urtishak, A. Asare, C.H. Bassing, and E.J. Brown. 2009. ATR and H2AX cooperate in maintaining genome stability under replication stress. *J. Biol. Chem.* 284:5994–6003. http://dx.doi.org/10.1074/jbc.M806739200

Clerici, M., V. Paciotti, V. Baldo, M. Romano, G. Lucchini, and M.P. Longhese. 2001. Hyperactivation of the yeast DNA damage checkpoint by TEL1 and DDC2 overexpression. *EMBO J.* 20:6485–6498. http://dx.doi.org/10.1093/emboj/20.22.6485

Corda, Y., S.E. Lee, S. Guillot, A. Walther, J. Sollier, A. Arbel-Eden, J.E. Haber, and V. Géli. 2005. Inactivation of Ku-mediated end joining suppresses *mec1*Δ lethality by depleting the ribonucleotide reductase inhibitor Sml1 through a pathway controlled by Tel1 kinase and the Mre11 complex. *Mol. Cell. Biol.* 25:10652–10664. http://dx.doi.org/10.1128/MCB.25.23.10652-10664.2005

Durkin, S.G., and T.W. Glover. 2007. Chromosome fragile sites. *Annu. Rev. Genet.* 41:169–192. http://dx.doi.org/10.1146/annurev.genet.41.042007.165900

Eckert-Boulet, N., R. Rothstein, and M. Lisby. 2011. Cell biology of homologous recombination in yeast. *Methods Mol. Biol.* 745:523–536. http://dx.doi.org/10.1007/978-1-61779-129-1_30

Gandhi, M., L.W. Dillon, S. Pramanik, Y.E. Nikiforov, and Y.H. Wang. 2010. DNA breaks at fragile sites generate oncogenic RET/PTC rearrangements in human thyroid cells. *Oncogene*. 29:2272–2280. http://dx.doi.org/10.1038/onc.2009.502

Germann, S.M., V.H. Oestergaard, C. Haas, P. Salis, A. Motegi, and M. Lisby. 2011. Dpb11/TopBP1 plays distinct roles in DNA replication, checkpoint response and homologous recombination. *DNA Repair (Amst.)*. 10:210–224. http://dx.doi.org/10.1016/j.dnarep.2010.11.001

Goedhart, J., L. van Weeren, M.A. Hink, N.O. Vischer, K. Jalink, and T.W. Gadella Jr. 2010. Bright cyan fluorescent protein variants identified by fluorescence lifetime screening. *Nat. Methods*. 7:137–139. http://dx.doi.org/10.1038/nmeth.1415

Goedhart, J., D. von Stetten, M. Noirclerc-Savoye, M. Lelimousin, L. Joosen, M.A. Hink, L. van Weeren, T.W. Gadella Jr., and A. Royant. 2012. Structure-guided evolution of cyan fluorescent proteins towards a quantum yield of 93%. *Nat Commun*. 3:751. http://dx.doi.org/10.1038/ncomms1738

Heim, R., and R.Y. Tsien. 1996. Engineering green fluorescent protein for improved brightness, longer wavelengths and fluorescence resonance energy transfer. *Curr. Biol.* 6:178–182. http://dx.doi.org/10.1016/S0960-9822(02)00450-5

Hirano, T., S. Funahashi, T. Uemura, and M. Yanagida. 1986. Isolation and characterization of *Schizosaccharomyces pombe* cutmutants that block nuclear division but not cytokinesis. *EMBO J.* 5:2973–2979.

James, P., J. Halladay, and E.A. Craig. 1996. Genomic libraries and a host strain designed for highly efficient two-hybrid selection in yeast. *Genetics*. 144:1425–1436.

Johnson, M., H.H. Phua, S.C. Bennett, J.M. Spence, and C.J. Farr. 2009. Studying vertebrate topoisomerase 2 function using a conditional knockdown system in DT40 cells. *Nucleic Acids Res.* 37:e98. http://dx.doi.org/10.1093/nar/gkp480

Kaulich, M., F. Cubizolles, and E.A. Nigg. 2012. On the regulation, function, and localization of the DNA-dependent ATPase PICH. *Chromosoma*. 121:395–408. http://dx.doi.org/10.1007/s00412-012-0370-0

Kegel, A., H. Betts-Lindroos, T. Kanno, K. Jeppsson, L. Ström, Y. Katou, T. Itoh, K. Shirahige, and C. Sjögren. 2011. Chromosome length influences replication-induced topological stress. *Nature*. 471:392–396. http://dx.doi.org/10.1038/nature09791

Keppler-Ross, S., C. Noffz, and N. Dean. 2008. A new purple fluorescent color marker for genetic studies in *Saccharomyces cerevisiae* and *Candida albicans*. *Genetics*. 179:705–710. http://dx.doi.org/10.1534/genetics.108.087080

Kumagai, A., J. Lee, H.Y. Yoo, and W.G. Dunphy. 2006. TopBP1 activates the ATR-ATRIP complex. *Cell*. 124:943–955. http://dx.doi.org/10.1016/j.cell.2005.12.041

Lahkim Bennani-Belhaj, K., S. Rouzeau, G. Buhagiar-Labarchède, P. Chabosseau, R. Onclercq-Delic, E. Bayart, F. Cordelières, J. Couturier, and M. Amor-Guéret. 2010. The Bloom syndrome protein limits the lethality associated with RAD51 deficiency. *Mol. Cancer Res.* 8:385–394. http://dx.doi.org/10.1158/1541-7786.MCR-09-0534

Laulier, C., A. Cheng, and J.M. Stark. 2011. The relative efficiency of homology-directed repair has distinct effects on proper anaphase chromosome separation. *Nucleic Acids Res.* 39:5935–5944. http://dx.doi.org/10.1093/nar/gkr187

Lea, D.E., and C.A. Coulson. 1949. The distribution in the numbers of mutants in bacterial populations. *J. Genet.* 49:264–285. http://dx.doi.org/10.1007/BF02986080

Liberi, G., G. Maffioletti, C. Lucca, I. Chiolo, A. Baryshnikova, C. Cotta-Ramusino, M. Lopes, A. Pellicioli, J.E. Haber, and M. Foiani. 2005. Rad51-dependent DNA structures accumulate at damaged replication forks in sgs1 mutants defective in the yeast ortholog of BLM RecQ helicase. *Genes Dev.* 19:339–350. http://dx.doi.org/10.1101/gad.322605

Lindsey-Boltz, L.A., and A. Sancar. 2011. Tethering DNA damage checkpoint mediator proteins topoisomerase IIbeta-binding protein 1 (TopBP1) and Claspin to DNA activates ataxia-telangiectasia mutated and RAD3-related (ATR) phosphorylation of checkpoint kinase 1 (Chk1). *J. Biol. Chem.* 286:19229–19236. http://dx.doi.org/10.1074/jbc.M111.237958

Lisby, M., J.H. Barlow, R.C. Burgess, and R. Rothstein. 2004. Choreography of the DNA damage response: spatiotemporal relationships among checkpoint and repair proteins. *Cell*. 118:699–713. http://dx.doi.org/10.1016/j.cell.2004.08.015

Lopes, M., C. Cotta-Ramusino, G. Liberi, and M. Foiani. 2003. Branch migrating sister chromatid junctions form at replication origins through Rad51/Rad52-independent mechanisms. *Mol. Cell*. 12:1499–1510. http://dx.doi.org/10.1016/S1097-2765(03)00473-8

Lucas, I., and O. Hyrien. 2000. Hemicatenanes form upon inhibition of DNA replication. *Nucleic Acids Res.* 28:2187–2193. http://dx.doi.org/10.1093/nar/28.10.2187

Lukas, C., V. Savic, S. Bekker-Jensen, C. Doil, B. Neumann, R.S. Pedersen, M. Grøfte, K.L. Chan, I.D. Hickson, J. Bartek, and J. Lukas. 2011. 53BP1 nuclear bodies form around DNA lesions generated by mitotic transmission of chromosomes under replication stress. *Nat. Cell Biol.* 13:243–253. http://dx.doi.org/10.1038/ncb2201

Mäkiniemi, M., T. Hillukkala, J. Tuusa, K. Reini, M. Vaara, D. Huang, H. Pospiech, I. Majuri, T. Westerling, T.P. Mäkelä, and J.E. Syväoja. 2001. BRCT domain-containing protein TopBP1 functions in DNA replication and damage response. *J. Biol. Chem.* 276:30399–30406. http://dx.doi.org/10.1074/jbc.M102245200

Matos, J., M.G. Blanco, and S.C. West. 2013. Cell-cycle kinases coordinate the resolution of recombination intermediates with chromosome segregation. *Cell Rep*. 4:76–86. http://dx.doi.org/10.1016/j.celrep.2013.05.039

Meister, P., A. Taddei, L. Vernis, M. Poidevin, S.M. Gasser, and G. Baldacci. 2005. Temporal separation of replication and recombination requires the intra-S checkpoint. *J. Cell Biol.* 168:537–544. http://dx.doi.org/10.1083/jcb.200410006

Mendoza, M., C. Norden, K. Durrer, H. Rauter, F. Uhlmann, and Y. Barral. 2009. A mechanism for chromosome segregation sensing by the NoCut checkpoint. *Nat. Cell Biol.* 11:477–483. http://dx.doi.org/10.1038/ncb1855

Mordes, D.A., E.A. Nam, and D. Cortez. 2008. Dpb11 activates the Mec1-Ddc2 complex. *Proc. Natl. Acad. Sci. USA*. 105:18730–18734. http://dx.doi.org/10.1073/pnas.0806621105

Naim, V., and F. Rosselli. 2009. The FANC pathway and BLM collaborate during mitosis to prevent micro-nucleation and chromosome abnormalities. *Nat. Cell Biol.* 11:761–768. http://dx.doi.org/10.1038/ncb1883

Naim, V., T. Wilhelm, M. Debatisse, and F. Rosselli. 2013. ERCC1 and MUS81-EME1 promote sister chromatid separation by processing late replication intermediates at common fragile sites during mitosis. *Nat. Cell Biol.* 15:1008–1015. http://dx.doi.org/10.1038/ncb2793

Nishimura, K., T. Fukagawa, H. Takisawa, T. Kakimoto, and M. Kanemaki. 2009. An auxin-based degron system for the rapid depletion of proteins in nonplant cells. *Nat. Methods*. 6:917–922. http://dx.doi.org/10.1038/nmeth.1401

Ormö, M., A.B. Cubitt, K. Kallio, L.A. Gross, R.Y. Tsien, and S.J. Remington. 1996. Crystal structure of the *Aequorea victoria* green fluorescent protein. *Science*. 273:1392–1395. http://dx.doi.org/10.1126/science.273.5280.1392

Pfander, B., and J.F. Diffley. 2011. Dpb11 coordinates Mec1 kinase activation with cell cycle-regulated Rad9 recruitment. *EMBO J.* 30:4897–4907. http://dx.doi.org/10.1038/emboj.2011.345

Porter, A.C., and C.J. Farr. 2004. Topoisomerase II: untangling its contribution at the centromere. *Chromosome Res.* 12:569–583. http://dx.doi.org/10.1023/B:CHRO.0000036608.91085.d1

Reini, K., L. Uitto, D. Perera, P.B. Moens, R. Freire, and J.E. Syväoja. 2004. TopBP1 localises to centrosomes in mitosis and to chromosome cores in meiosis. *Chromosoma*. 112:323–330. http://dx.doi.org/10.1007/s00412-004-0277-5

Schramke, V., H. Neecke, V. Brevet, Y. Corda, G. Lucchini, M.P. Longhese, E. Gilson, and V. Géli. 2001. The set1Delta mutation unveils a novel signaling pathway relayed by the Rad53-dependent hyperphosphorylation of replication protein A that leads to transcriptional activation of repair genes. *Genes Dev.* 15:1845–1858. http://dx.doi.org/10.1101/gad.193901

Shaner, N.C., R.E. Campbell, P.A. Steinbach, B.N. Giepmans, A.E. Palmer, and R.Y. Tsien. 2004. Improved monomeric red, orange and yellow fluorescent proteins derived from *Discosoma* sp. red fluorescent protein. *Nat. Biotechnol.* 22:1567–1572. http://dx.doi.org/10.1038/nbt1037

Sherman, F. 2002. Getting started with yeast. *Methods Enzymol.* 350:3–41. http://dx.doi.org/10.1016/S0076-6879(02)50954-X

Sikorski, R.S., and P. Hieter. 1989. A system of shuttle vectors and yeast host strains designed for efficient manipulation of DNA in *Saccharomyces cerevisiae. Genetics*. 122:19–27.

Silva, S., I. Gallina, N. Eckert-Boulet, and M. Lisby. 2012. Live cell microscopy of DNA damage response in *Saccharomyces cerevisiae*. *Methods Mol. Biol.* 920:433–443. http://dx.doi.org/10.1007/978-1-61779-998-3_30

Smith, J., and R. Rothstein. 1995. A mutation in the gene encoding the *Saccharomyces cerevisiae* single-stranded DNA-binding protein Rfa1 stimulates a *RAD52*-independent pathway for direct-repeat recombination. *Mol. Cell. Biol.* 15:1632–1641.

Sofueva, S., F. Osman, A. Lorenz, R. Steinacher, S. Castagnetti, J. Ledesma, and M.C. Whitby. 2011. Ultrafine anaphase bridges, broken DNA and illegitimate recombination induced by a replication fork barrier. *Nucleic Acids Res.* 39:6568–6584. http://dx.doi.org/10.1093/nar/gkr340

Spence, J.M., H.H. Phua, W. Mills, A.J. Carpenter, A.C. Porter, and C.J. Farr. 2007. Depletion of topoisomerase IIalpha leads to shortening of the metaphase interkinetochore distance and abnormal persistence of PICH-coated anaphase threads. *J. Cell Sci.* 120:3952–3964. http://dx.doi.org/10.1242/jcs.013730

Steigemann, P., C. Wurzenberger, M.H. Schmitz, M. Held, J. Guizetti, S. Maar, and D.W. Gerlich. 2009. Aurora B-mediated abscission checkpoint protects against tetraploidization. *Cell*. 136:473–484. http://dx.doi.org/10.1016/j.cell.2008.12.020

Struhl, K., D.T. Stinchcomb, S. Scherer, and R.W. Davis. 1979. High-frequency transformation of yeast: autonomous replication of hybrid DNA molecules. *Proc. Natl. Acad. Sci. USA*. 76:1035–1039. http://dx.doi.org/10.1073/pnas.76.3.1035

Szakal, B., and D. Branzei. 2013. Premature Cdk1/Cdc5/Mus81 pathway activation induces aberrant replication and deleterious crossover. *EMBO J.* 32:1155–1167. http://dx.doi.org/10.1038/emboj.2013.67

Tercero, J.A., and J.F. Diffley. 2001. Regulation of DNA replication fork progression through damaged DNA by the Mec1/Rad53 checkpoint. *Nature*. 412:553–557. http://dx.doi.org/10.1038/35087607

Toledo, L.I., M. Murga, R. Zur, R. Soria, A. Rodriguez, S. Martinez, J. Oyarzabal, J. Pastor, J.R. Bischoff, and O. Fernandez-Capetillo. 2011. A cell-based screen identifies ATR inhibitors with synthetic lethal properties for cancer-associated mutations. *Nat. Struct. Mol. Biol.* 18:721–727. http://dx.doi.org/10.1038/nsmb.2076

Torres-Rosell, J., F. Machín, A. Jarmuz, and L. Aragón. 2004. Nucleolar segregation lags behind the rest of the genome and requires Cdc14p activation by the FEAR network. *Cell Cycle*. 3:496–502. http://dx.doi.org/10.4161/cc.3.4.802

Viggiani, C.J., and O.M. Aparicio. 2006. New vectors for simplified construction of BrdU-Incorporating strains of *Saccharomyces cerevisiae*. *Yeast*. 23:1045–1051. http://dx.doi.org/10.1002/yea.1406

Vinciguerra, P., S.A. Godinho, K. Parmar, D. Pellman, and A.D. D'Andrea. 2010. Cytokinesis failure occurs in Fanconi anemia pathway-deficient murine and human bone marrow hematopoietic cells. *J. Clin. Invest.* 120:3834–3842. http://dx.doi.org/10.1172/JCI43391

Wang, L.H., B. Mayer, O. Stemmann, and E.A. Nigg. 2010. Centromere DNA decatenation depends on cohesin removal and is required for mammalian cell division. *J. Cell Sci.* 123:806–813. http://dx.doi.org/10.1242/jcs.058255

Wellinger, R.E., P. Schär, and J.M. Sogo. 2003. Rad52-independent accumulation of joint circular minichromosomes during S phase in *Saccharomyces cerevisiae*. *Mol. Cell. Biol.* 23:6363–6372. http://dx.doi.org/10.1128/MCB.23.18.6363-6372.2003

Wu, L., and I.D. Hickson. 2003. The Bloom's syndrome helicase suppresses crossing over during homologous recombination. *Nature*. 426:870–874. http://dx.doi.org/10.1038/nature02253

Wyatt, H.D., S. Sarbajna, J. Matos, and S.C. West. 2013. Coordinated Actions of SLX1-SLX4 and MUS81-EME1 for Holliday Junction Resolution in Human Cells. *Mol. Cell*. 52:234–247. http://dx.doi.org/10.1016/j.molcel.2013.08.035

Yamane, K., M. Kawabata, and T. Tsuruo. 1997. A DNA-topoisomerase-II-binding protein with eight repeating regions similar to DNA-repair enzymes and to a cell-cycle regulator. *Eur. J. Biochem.* 250:794–799. http://dx.doi.org/10.1111/j.1432-1033.1997.00794.x

Ying, S., S. Minocherhomji, K.L. Chan, T. Palmai-Pallag, W.K. Chu, T. Wass, H.W. Mankouri, Y. Liu, and I.D. Hickson. 2013. MUS81 promotes common fragile site expression. *Nat. Cell Biol.* 15:1001–1007. http://dx.doi.org/10.1038/ncb2773